Springer

KSME

Journal of Mechanical Science and Technology 32 (11) (2018) 5373~5387
www.springerlink.com/content/1738-494x(Print)/1976-3824(Online)
DOI 10.1007/s12206-018-1036-5

Task-oriented type synthesis of the lower-mobility parallel mechanisms with a common platform †

Byung-Ju Yi[1] and Whee Kuk Kim[2,*]

[1]*Department of Electronic Systems Engineering, Hanyang University, Ansan, Korea*
[2]*Department of Electro-Mechanical System Engineering, Korea University, Sejong, Korea*

(Manuscript Received August 7, 2017; Revised June 15, 2018; Accepted July 18, 2018)

Abstract

A systematic procedure for the task-oriented type synthesis of parallel mechanisms (PMs) with a common platform is proposed in this study. The method is composed of two stages. In the first stage, constraint wrenches that are compatible to specific task-oriented output motions of the PM is distributed to several limbs. In the second stage, the geometric conditions and admissible joint structures of PM limbs are identified by employing the concept of reciprocal screw. Then desired symmetric or asymmetric PMs are constructed with the proper combinations of those admissible limbs. Lastly, the suggested synthesis method is verified by identifying various forms of lower-mobility PMs, such as planar 1T-type PMs, spatial 2T-type PMs and spatial 1T2R-type PMs.

Keywords: Lower mobility; Parallel mechanism; Screw theory; Synthesis; Task-oriented

1. Introduction

The parallel mechanism (PM) has been known to have advantages over the serial mechanism in aspects of rigidity, precision, and low inertia, etc. Thus, numerous efforts have been made to conceive various useful structures of the PMs, whether symmetric or asymmetric [1-13].

Typical structures of the PMs are usually composed of the base plate, the upper plate, and several limbs connecting those two plates. When the PM employs identical limbs only, it is called symmetric. Otherwise, it is called asymmetric. Lower-mobility PMs denote those with less than 6 operational degrees of freedom (DOFs) in their upper plate. Less DOF motions of those lower mobility PMs are secured by the constraints imposed by the limbs. Thus, the objective of the synthesis method of the lower-mobility PMs is to effectively identify admissible joint types and structures for various types of constrained limbs. There are two typical approaches for the synthesis of the PMs: the constraint screw and Lie groups of displacement. Brief summary on previous works are summarized as follows.

Huang and Li [1, 2] suggested a type synthesis method employing the constraint screws and investigated joint types for various types of symmetric lower-mobility PMs. Gao et al. [3] suggested several types of composite pairs and new types of sub-chain; they conducted Plücker-coordinates-based type synthesis to introduce various lower-mobility PMs employing their suggested pairs and sub-chains. Fang and Tsai [4] focused on two different types of limb constraints, namely, a zero-pitch constraint limb and an infinite-pitch constraint limb; they conducted type synthesis of 4-DOF and 5-DOF PMs with identical limb structures.

Kong and Gosselin [5] also conducted type synthesis of the PMs based on screw theory. They employed the virtual chain approach. The procedure in the virtual chain approach can be divided into three main steps: i) Decomposition of the wrench systems of the parallel kinematic chain including the desired virtual chain, ii) type synthesis of limbs, and iii) assembly of the limbs to generate the PM.

Li et al. [6] suggested a synthesis method employing algebraic properties of the Lie groups of displacement and introduced new structures of various lower-mobility PMs. Karouia and Hervé [7] conducted on the type synthesis of the asymmetrical and non-over-constrained spherical 3-DOF PMs based on the Lie group theory. Refaat et al. [8] suggested four families of the asymmetrical and rotational–translational 3-DOF PMs (two $1T2R$ families and two $2T1R$ families) based on Lie group theory, where $mTnR$ denotes m-DOF translational output motion and n-DOF rotational output motion of the PM. Salgado et al. [9] conducted type synthesis of $3T1R$ -type PMs with Schönflies motion employing the method of Lie group of displacement; they identified various $3T1R$ -type symmetric PMs employing revolute joints, pris-

*Corresponding author. Tel.: +82 44 860 1443, Fax.: +82 44 865 1820
E-mail address: wheekuk@korea.ac.kr
† Recommended by Associate Editor Hugo Rodrigue

matic joints and planar parallelograms. Lee and Hervé [10] conducted type synthesis including helical joints in addition to revolute and prismatic joints and planar parallelograms; they suggested various forms of $3T1R$ PMs with Schönflies motion.

Along with those works on the type synthesis of the PMs, there have been many other efforts to identify various types of symmetric or asymmetric PMs both with high performance and with application potential in industry. Yi et al. [11] suggested an asymmetrical $3T1R$ PM which could be applicable in multi-task operations by slight modifications. Chung et al. [14] suggested a $1T2R$-type 3-DOF asymmetric PM and employed it as a flat-panel TV mounting device; they also suggested a new $1T2R$-type symmetric PMs [15] and used the foldable 3-DOF PM as a master device to control the robot in perform the glass window panel fitting task in a building construction field. Kim et al. [16] employed an asymmetric PM structure to the design of the $3T1R$ type 4-DOF haptic device.

Affluent structures of the symmetric and the asymmetric lower-mobility PMs based on the Lie groups of displacement has been reported so far. However, most of the previous works on the type synthesis of the PMs employing the constraint screw have focused on the identification the admissible limb structures for the selected output motion DOFs of the symmetric PMs. In fact, the synthesis method based on the constraint screw has advantages for the synthesis of the PM with target-oriented motion DOFs since any mechanism constraints could be effectively distributed to its limbs. However, no systematic and comprehensive approach has been addressed to effectively identify both symmetric and asymmetric PMs with any target-oriented motion DOFs. Thus, more works should be done to identify the novel and practical structures of the symmetric/asymmetric PMs.

In this work, a systematic procedure for the task-oriented type synthesis of the PMs, whether symmetric or asymmetric, is proposed based on the constraint screws. For simplicity, the type synthesis for various lower-mobility PMs which has a common platform and employs the revolute and/or prismatic joints only is conducted. Note that the same procedure could be applied to the type synthesis of the PMs employing other joint types (e.g., universal, spherical, cylindrical, and helical joints) and any other generalized pairs (e.g., planar parallelograms), which can be treated as a generalized kinematic pair with 1-DOF translational motion.

Note that the suggested approach is similar to the one in the virtual chain approach except the first step i) where all types of constraint wrenches of the limbs are identified by employing the virtual chain concept. In suggested approach, all the constraint wrenches of the limb are identified by distributing both all the constraint wrenches of the PM and the ones equivalent to those of the PM to limbs, directly. Note that since all constraint wrenches of limbs of the PM are expressed with respect to the same output reference frame of the PM, the concept of "virtual chain" is not required in the task-oriented synthesis method suggested in this study and also the limb structures with various forms of constraint wrenches could be directly employed to the syntheses for any other task-oriented PMs as will be illustrated in this work. In these aspects, the synthesis method suggested in this work is comprehensive and systematic as the virtual chain approach but simpler and easier to apply than the virtual chain approach.

This paper is organized as follows. Sec. 2 describes the screw theory briefly and then introduces the task-oriented type synthesis procedure, which is applicable to the PMs with a common platform. Sec. 3 briefly addresses mechanism constraints of the PM in task-space and various types of constrained limbs. Sec. 4 shows the procedures of identifying the joint structures for various forms of limbs which are characterized by different sets of constraint wrenches. Sec. 5 describes the procedure of the task-oriented type synthesis via three different types of lower-mobility PMs (i.e., planar $1T_{y^*}$, spatial $2T_{x^*y^*}$, and spatial $1T_{z^*}2R_{x^*y^*}$ types) and presents some new PM structures. Sec. 6 concludes the paper.

2. Task-oriented type synthesis method

2.1 Screw theory

Screw coordinates have advantages over the other 3D vector-based coordinates. They can be used to describe either the translational and rotational motions of an object or the resultant force and torque applied to the object altogether. A screw is divided into two types, namely, twist or wrench, depending on different physical quantities employed. Twist is related to translational and rotational motions, whereas wrench is related to resultant force and torque. Twist and wrench are defined, respectively, as

$$\$_T = \begin{pmatrix} \omega\hat{\boldsymbol{s}}_T & \boldsymbol{r}_T \times \omega\hat{\boldsymbol{s}}_T + v\hat{\boldsymbol{s}}_T \end{pmatrix} = \omega\begin{pmatrix} \hat{\boldsymbol{s}}_T & \boldsymbol{r}_T \times \hat{\boldsymbol{s}}_T + \lambda_T\hat{\boldsymbol{s}}_T \end{pmatrix} = \omega\hat{\$}_T \,, \tag{1}$$

$$\$_W = \begin{pmatrix} f\hat{\boldsymbol{s}}_W & \boldsymbol{r}_W \times f\hat{\boldsymbol{s}}_W + \tau\hat{\boldsymbol{s}}_W \end{pmatrix} = f\begin{pmatrix} \hat{\boldsymbol{s}}_W & \boldsymbol{r}_W \times \hat{\boldsymbol{s}}_W + \lambda_W\hat{\boldsymbol{s}}_W \end{pmatrix} = f\hat{\$}_W, \tag{2}$$

where $\hat{\boldsymbol{s}}_T$ and $\hat{\boldsymbol{s}}_W$ denote the unit vectors along the corresponding screw axis, $\boldsymbol{r}_T$ and $\boldsymbol{r}_W$ are the position vectors from the origin of the reference frame to the corresponding screw axes, ω is the angular rate, v is the translational speed, f is the magnitude of force, and τ denotes the magnitude of torque at the origin of the reference frame. The reference frame can be defined as a body fixed frame that has its origin at the point of interest of the body. λ_T and λ_W denote the twist pitch defined as $\lambda_T = v/\omega$ and the wrench pitch defined as $\lambda_W = \tau/f$, respectively. $\hat{\$}_T$ and $\hat{\$}_W$ denote the unit screws. In particular, the unit screw for the revolute joint, which is a zero-pitch twist, is expressed as $\hat{\$} = \begin{pmatrix} \hat{\boldsymbol{s}} & \boldsymbol{r} \times \hat{\boldsymbol{s}} \end{pmatrix}$, and the unit screw for the prismatic joint, which is an infinite-pitch twist, is expressed as $\hat{\$} = \begin{pmatrix} \boldsymbol{0} & \hat{\boldsymbol{s}} \end{pmatrix}$.

The orthogonal product operation between the twist and the wrench is defined as follows:

Table 1. Cases of zero-orthogonal products.

Case	Feature
1	The orthogonal product between two arbitrary zero-pitch screws is zero.
2	The orthogonal product between zero-pitch and infinite-pitch screws is zero.
3	The orthogonal product between two arbitrary infinite-pitch screws is zero.

$$\begin{aligned}\hat{\$}_W \circ \hat{\$}_T &= \left(\hat{\boldsymbol{s}}_W \quad \boldsymbol{r}_W \times \hat{\boldsymbol{s}}_W + \lambda_W \hat{\boldsymbol{s}}_W\right) \circ \left(\hat{\boldsymbol{s}}_T \quad \boldsymbol{r}_T \times \hat{\boldsymbol{s}}_T + \lambda_T \hat{\boldsymbol{s}}_T\right) \\ &= \hat{\boldsymbol{s}}_W \cdot (\boldsymbol{r}_T \times \hat{\boldsymbol{s}}_T + \lambda_T \hat{\boldsymbol{s}}_T) + (\boldsymbol{r}_W \times \hat{\boldsymbol{s}}_W + \lambda_W \hat{\boldsymbol{s}}_W) \cdot \hat{\boldsymbol{s}}_T\end{aligned}, \tag{3}$$

where "$\circ$" denotes the orthogonal product operator. The result of Eq. (3) represents the power transmitted through the twist and wrench. The condition that the result of the orthogonal product operation becomes zero implies that the transmitted power through these screw pairs becomes zero. When this condition is met, the twist and wrench are called "reciprocal".

Table 1 shows three typical cases in which the orthogonal product between two different types of screws (i.e., zero-pitch and infinite-pitch screws) becomes zero. The geometric conditions for these three cases of orthogonal products that are needed to effectively identify the admissible joint types and structures for various types of constrained limbs are employed in Sec. 4. Thus, detailed derivations and interpretations for geometrical conditions corresponding to those three cases are discussed in this section.

Case 1. The condition that the orthogonal product between two arbitrary zero-pitch wrench and twist screws becomes zero can be written as follows:

$$\begin{aligned}\hat{\$}_W \circ \hat{\$}_T &= \left(\hat{\boldsymbol{s}}_W \quad \boldsymbol{r}_W \times \hat{\boldsymbol{s}}_W\right) \circ \left(\hat{\boldsymbol{s}}_T \quad \boldsymbol{r}_T \times \hat{\boldsymbol{s}}_T\right) \\ &= (\boldsymbol{r}_W - \boldsymbol{r}_T) \cdot \hat{\boldsymbol{s}}_W \times \hat{\boldsymbol{s}}_T = -a \sin\alpha = 0\end{aligned}, \tag{4}$$

where a denotes the distance along the common normal axis of two screw axes, and α denotes the angle between two screw axes about the common normal axis, as shown in Fig. 1. Thus, geometric conditions for those two screws to be reciprocal to each other can be identified as

(a) $\sin\alpha = 0$ (i.e., $\hat{\boldsymbol{s}}_W$ and $\hat{\boldsymbol{s}}_T$ are parallel)

or

(b) $a = 0$ (i.e., $\hat{\boldsymbol{s}}_W$ and $\hat{\boldsymbol{s}}_T$ intersect).

Case 2. The orthogonal product between the zero-pitch and infinite-pitch screws can be written as

$$\hat{\$}_W \circ \hat{\$}_T = \left(\hat{\boldsymbol{s}}_W \quad \boldsymbol{r}_W \times \hat{\boldsymbol{s}}_W\right) \circ \left(0 \quad \hat{\boldsymbol{s}}_T\right) = \hat{\boldsymbol{s}}_W \cdot \hat{\boldsymbol{s}}_T = 0\,. \tag{5}$$

Thus, the geometric condition that the orthogonal product between those two screws becomes zero is that two screw axes are orthogonal.

Case 3. The condition that the orthogonal product between the two infinite-pitch screws becomes zero is none because

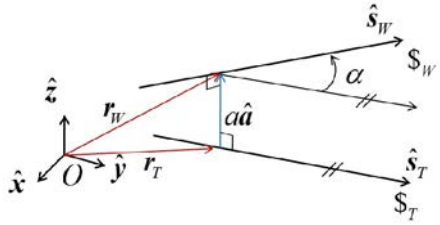

Fig. 1. Geometry of two screw axes.

$$\hat{\$}_W \circ \hat{\$}_T = \left(\boldsymbol{0} \quad \hat{\boldsymbol{s}}_W\right) \circ \left(\boldsymbol{0} \quad \hat{\boldsymbol{s}}_T\right) = 0\,. \tag{6}$$

Thus, any infinite twist is reciprocal to the infinite wrench or vice versa.

The concept of "reciprocity" has been employed effectively in the constraint-screw-based synthesis of the PMs [1, 2, 4]. Several terminologies related to the constraint-screw-based synthesis are defined as follows. An output motion screw system of the PM is defined as the set composed of independent motion screws of the PM and is denoted as $\{\$_M\} = \{\$_{M1}, \$_{M2}, \cdots, \$_{Mn}\}$, where n is the DOF of the PM. An output constraint screw system of the PM defined as $\{\$^r_M\} = \{\$^r_{M1}, \$^r_{M2}, \cdots, \$^r_{M(6-n)}\}$ represents the set containing all independent constraint wrenches imposed on the moving plate of the PM. Any twist in the output motion screw system of the PM is reciprocal to all wrenches of its output constraint screw system. Therefore, $\dim\{\$_M\} + \dim\{\$^r_M\} = 6$ always holds.

Similarly, the limb motion screw system defined as $\{\$_L\} = \{\$_{L1}, \$_{L2}, \cdots, \$_{Ln}\}$ denotes the set consisting of the independent joint screws of the limb. A limb constraint wrench system defined as $\{\$^r_L\} = \{\$^r_{L1}, \$^r_{L2}, \cdots, \$^r_{L(6-n)}\}$ represents the set composed of all independent constraint wrenches. Moreover, $\dim\{\$_L\} + \dim\{\$^r_L\} = 6$ always holds. Any screw in a limb constraint wrench system is reciprocal to all joint screws of the limb. Hereafter, the reference frame of all the screws is fixed to the moving plate of the PM.

2.2 Type synthesis procedure

For simplicity, the following three assumptions are imposed on the type synthesis in this study.

(i) The PM consists of a common platform with several limbs.

(ii) The PM employs only two different types of joints, namely, revolute joint and/or prismatic joint.

(iii) Each limb is a serial type and has no kinematic redundancy.

The type synthesis method suggested in this study consists of two stages. In the first stage, constraint wrenches that are compatible to the task-oriented output motions of the PM is distributed to several limbs. In the second stage, the geometric conditions and the admissible joint structures of the constrained limbs are identified by employing the concept of reciprocal screw. Then desired symmetric and/or asymmetric PMs are constructed with the proper combinations of those

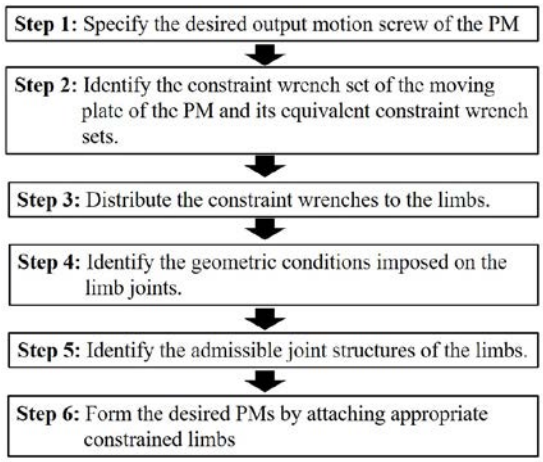

Fig. 2. Summary of the proposed synthesis procedure.

admissible limbs. Fig. 2 shows the summary of the proposed synthesis procedure:

And its detailed synthesis steps are described one by one as follows.

First stage:

The first stage of the synthesis procedure can be divided into three steps, which are summarized as follows.

Step 1. Specify the desired output motion screw

The desired output motion screws of the PM are specified as ($\{\$_M\}=\{\$_{M1},\$_{M2},\cdots,\$_{Mn}\}$), where n denotes the DOF of the PM; and $\$_{M1}$, $\$_{M2}\cdots$, $\$_{Mn}$ denote the desired output motion screws. The desired output motion can be expressed with respect to either the non-rotating reference frame or rotating reference frame. In the following, any symbol with * as its superscript denotes that it is expressed with respect to the rotating reference frame.

Step 2. Identify the constraint wrench set of the moving plate of the PM and its equivalent constraint wrench sets

The constraint wrenches imposed on the moving plate of the PM (i.e., $\{\$^r_M\}=\{\$^r_{M1},\$^r_{M2},\cdots,\$^r_{M(6-n)}\}$) are identified from its desired output motion screws, using the reciprocal screw conditions (i.e., $\$^r_{Mi}\circ\$_{Mj}=0,\quad \forall\, i=1,2,\cdots,n,\quad j=1,2,\cdots,(6-n).$). The equivalent constraint wrench sets to those constraint wrenches, if any, are also identified in this step.

Step 3. Distribute the constraint wrenches to the limbs

Each of the constraint wrench set of the PM including its equivalent constraint wrench sets are distributed appropriately to the limbs (i.e., $\{\$^r_{LN}\}$ *for* $N=1,2,\cdots N_s$, where N_s is the number of the limbs). The dimension of all constraint wrenches from all limbs (i.e., $Rank(\{\$^r_{L1}\},\{\$^r_{L2}\},\cdots,\{\$^r_{LN}\})$) should be equal to $(6-n)$. If the mechanism constraint wrenches are distributed to the limbs without duplication, the total number of the constraint wrenches is $(6-n)$. Subsequently, the PM becomes non-over-constrained. If the total number of the constraint wrenches distributed to the limbs is greater than $(6-n)$, then the PM becomes over-constrained. Notably, the PM tends to have less joints when it becomes more over-constrained, thereby increasing its stiffness. Thus, more over-constrained PMs are preferable in most of practical applications. For example, a planar 3-DOF PM is an example of over-constrained PM in spatial domain which has 3 over-constraints while it can be seen as a non-over-constrained PM in planar domain. When those three over-constraints are removed, the stiffness along the directions of those three removed over-constraints becomes lower.

Second Stage:

The second stage of the synthesis procedure can be divided into three steps, which are summarized as follows.

Step 4. Identify the geometric conditions imposed on the limb joints

The geometric conditions imposed on the limbs are identified by examining the reciprocal conditions to the limb constraint wrenches, which are assigned to each of the limbs in step 3.

Step 5. Identify the admissible joint structures of the limbs

The admissible joint structures of the limbs can be identified based on the geometric conditions in step 4, and their full cycle in mobility (FCIM) is checked. Note that the motion of the proximal revolute joint of the serial limb can change the axis directions of the distal joints. Therefore, the FCIM of the admissible limbs can be tested by checking whether or not the geometric conditions imposed on those admissible joints (i.e., directions of the distal joint axes) are violated by finite displacements of the other proximal revolute joints placed toward the ground.

Step 6. Identity the desired PMs

Various forms of PMs (i.e., symmetric or asymmetric) can be constructed with the proper combination of the limbs identified. However, care must be taken in selecting constrained limbs with respect to the rotating reference frame not to lose the FCIM during its motion.

The geometric conditions for various types of constrained limbs and their admissible joint structures in steps 4~6, can be identified in advance, noting that they could be employed repeatedly in various task-oriented structure syntheses. Thus, in the following section, types of constrained limbs and the limb constraint wrenches corresponding to the $mTnR$ type output motions of the PMs are discussed in detail.

3. Constrained limbs in a task-oriented space

3.1 Constrained limb types in task-oriented space

The PM consisting of several limbs is subject to the constraint wrenches imposed by the limbs. Those constrained limbs can be classified according to 1) the directions of the constraint wrench axes in the task-oriented frame (which is either non-rotating or rotating) and 2) their pitch types (i.e., zero-pitch or infinite-pitch. Thus, two different task-oriented frames are defined and employed. One frame $(\boldsymbol{x}^*,\boldsymbol{y}^*,\boldsymbol{z}^*)$ denotes the task-oriented rotating reference frame whose origin is fixed to the moving plate of the PM. The other frame

$(\boldsymbol{x},\boldsymbol{y},\boldsymbol{z})$ denotes the non-rotating task-oriented reference frame whose origin is coincident with the one of the rotating reference frame.

Table 2 shows the typical types of the constrained limbs with respect to those two task-oriented reference frames for the $mTnR$ type PMs. The types of the constrained limbs whose structures are analogous to one another are grouped together by the same parenthesis in the table. Notations are adopted such that the $F_{x^*y^*}C_{z^*}$-limb denotes the constrained limb, which provides the PM with two pure force constraints along the x- and y- directions of the rotating reference frame and with a pure couple constraint around the z- axis of the same rotating reference frame.

The $F_{x^*y^*}C_{z^*}$-limb can also be interpreted as a $1T_{z^*}2R_{x^*y^*}$ type 3-DOF limb. The $R_xR_yP_z$-type limb is one example of the $1T_{z^*}2R_{x^*y^*}$ type 3-DOF limb. Its output motion can be characterized as two consecutive rotations, the rotation about the x- axis of the non-rotating reference frame first and another rotation about the y- axis of the rotated frame, and then the 1- DOF translational motion along the z- axis of the resulting rotated frame. Note that F_{xyz} is equivalent to $F_{x^*y^*z^*}$ and C_{xyz} is equivalent to $C_{x^*y^*z^*}$ because those two force constraint domains and those two torque constraint domains cover the same 3-dimensional force domain or the same 3-dimensional torque constraint domain, respectively.

The constrained limbs, including one infinite-pitch constraint wrench with respect to the non-rotating reference frame only such as the C_z, F_zC_z, F_xC_z, $F_{xy}C_z$ and $F_{xy}C_x$ type constraints, are not included in Table 2 because they cannot be realized. Such constrained limbs are not fully cyclic in mobility because their geometric conditions are violated by the rotational motion of more than two proximal revolute joints.

By contrast, the constrained limbs, including two infinite-pitch constraint wrenches with respect to either the non-rotating reference frame or the rotating reference frame could be realized. For example, the C_{xy}-type and the $C_{x^*y^*}$-type constraints of the constrained limbs can be easily realized by R_z type revolute joint and R_{z^*} type revolute joint, respectively. Note that each axis of two R_z and R_{z^*} joints is parallel to the z- and z^*- axes, respectively. For simplicity, most of those realizable constrained limbs are included in Table 2. However, for simplicity, those limb constraint types, including two infinite-pitch constraint wrenches with respect to the non-rotating reference frame (e.g., C_{xy},C_{xz},C_{yz} types), are omitted.

Table 2. Types of constrained limbs.

Number of constraints	Types of constrained limbs
1	F_x, F_y, F_z; F_{x^*}, F_{y^*}, F_{z^*}; C_{x^*}, C_{y^*}, C_{z^*}
2	F_{xy}, F_{xz}, F_{yz}; $F_{x^*y^*}$, $F_{x^*z^*}$, $F_{y^*z^*}$; C_{xy}, C_{xz}, C_{yz}; $C_{x^*y^*}$, $C_{x^*z^*}$, $C_{y^*z^*}$; $F_{x^*}C_{x^*}$, $F_{y^*}C_{y^*}$, $F_{z^*}C_{z^*}$; $F_xC_{x^*}$, $F_yC_{y^*}$, $F_zC_{z^*}$; $F_{x^*}C_{y^*}$, $F_{y^*}C_{x^*}$, $F_{x^*}C_{z^*}$, $F_{z^*}C_{x^*}$, $F_{y^*}C_{z^*}$, $F_{z^*}C_{y^*}$; $F_xC_{y^*}$, $F_yC_{x^*}$, $F_xC_{z^*}$, $F_zC_{x^*}$, $F_yC_{z^*}$, $F_zC_{y^*}$
3	F_{xyz}, C_{xyz}; $F_{x^*}C_{y^*z^*}$, $F_{y^*}C_{x^*z^*}$, $F_{z^*}C_{x^*y^*}$; $F_xC_{y^*z^*}$, $F_yC_{x^*z^*}$, $F_zC_{x^*y^*}$; $F_{x^*}C_{x^*y^*}$, $F_yC_{y^*z^*}$, $F_zC_{y^*z^*}$; $F_{x^*y^*}C_{z^*}$, $F_{x^*z^*}C_{y^*}$, $F_{y^*z^*}C_{x^*}$; $F_{xy}C_{z^*}$, $F_{xz}C_{y^*}$, $F_{yz}C_{x^*}$; $F_{x^*y^*}C_{x^*}$, $F_{x^*y^*}C_{y^*}$, $F_{x^*z^*}C_{x^*}$, $F_{x^*z^*}C_{z^*}$, $F_{y^*z^*}C_{y^*}$, $F_{y^*z^*}C_{z^*}$; $F_{xy}C_{x^*}$, $F_{xy}C_{y^*}$, $F_{xz}C_{x^*}$, $F_{xz}C_{z^*}$, $F_{yz}C_{y^*}$, $F_{yz}C_{z^*}$
4	$F_{x^*y^*}C_{x^*y^*}$, $F_{y^*z^*}C_{y^*z^*}$, $F_{x^*z^*}C_{x^*z^*}$; $F_{xy}C_{x^*y^*}$, $F_{xz}C_{y^*z^*}$; $F_{x^*y^*}C_{y^*z^*}$, $F_{x^*y^*}C_{x^*z^*}$, $F_{x^*z^*}C_{x^*y^*}$, $F_{x^*z^*}C_{y^*z^*}$, $F_{y^*z^*}C_{x^*y^*}$, $F_{y^*z^*}C_{x^*z^*}$; $F_{xy}C_{y^*z^*}$, $F_{xy}C_{x^*z^*}$, $F_{xz}C_{x^*y^*}$, $F_{xz}C_{y^*z^*}$, $F_{yz}C_{x^*y^*}$, $F_{yz}C_{x^*z^*}$; $F_{x^*}C_{xyz}$, $F_{y^*}C_{xyz}$, $F_{z^*}C_{xyz}$; F_xC_{xyz}, F_yC_{xyz}, F_zC_{xyz}
5	$F_{xyz}C_{x^*y^*}$, $F_{xyz}C_{y^*z^*}$, $F_{xyz}C_{x^*z^*}$; $F_{x^*y^*}C_{xyz}$, $F_{y^*z^*}C_{xyz}$, $F_{x^*z^*}C_{xyz}$; $F_{xy}C_{xyz}$, $F_{yz}C_{xyz}$, $F_{xz}C_{xyz}$

Table 3. Limb output motions of the various planar PMs and the corresponding limb constraint wrenches.

Limb output motions of the planar PMs	Limb constraint wrenches in the planar domain	Limb constraint wrenches in the spatial domain
T_x	F_yR_z	$F_{yz}C_{xyz}$
T_{x^*}	$F_{y^*}R_z$	$F_{y^*z}C_{xyz}$
R_z	$F_{xy}=F_{x^*y^*}$	$F_{xyz}C_{xy}$
T_xR_z	F_y	$F_{yz}C_{xy}$
$T_{x^*}R_z$	F_{y^*}	$F_{y^*z}C_{xy}$
T_{xy} or $T_{x^*y^*}$	R_z	F_zC_{xyz}
$T_{xy}R_z$ or $T_{x^*y^*}R_z$	$\varnothing$	F_zC_{xy}

3.2 Constrained limb types and their constraint wrenches

In this section, the typical forms of the constrained limbs for the $mTnR$ type task-oriented space of the PMs are investigated in detail. In particular, the planar and spherical PMs are discussed before addressing the lower-mobility PMs in the spatial domain. Table 3 shows the limb output motions of the various planar PMs and the corresponding limb constraint wrenches in the planar and spatial domains. As before, T_x and T_{x^*} denote the 1-DOF translational motion along the x-axis of the non-rotating planar frame and along the x^*-axis which is the x- axis of the rotating planar frame, respectively. Note that T_{xy} and $T_{x^*y^*}$ in the plane domain are equivalent because they cover the same planar translational 2-DOF domain.

Table 4 shows the types of limb output motions of the various spherical PMs and the corresponding limb constraint wrenches in the spherical and spatial domains. As previously discussed, the constrained limbs with one infinite-pitch constraint wrench with respect to the axis of the non-rotating reference frame, such as the C_x-type constraint, are not realizable and thus excluded. Table 4 shows a few selected output motions of the spherical PMs. $R_{x^*y^*z^*}$ denotes the rotational 3-DOF motion that can be realized by any three independent angle sets.

Table 5 shows the various limb output motions of the $mTnR$ type lower-mobility PMs in the spatial domain and

Table 4. Limb output motions of the spherical PMs and their corresponding limb constraint wrenches.

Limb output Motion of the spherical PM	Limb constraint wrenches in spherical domain	Limb constraint wrenches in spatial domain
R_x	C_{yz}	$F_{xyz}C_{yz}$
R_{x^*}	$C_{y^*z^*}$	$F_{xyz}C_{y^*z^*}$
$R_{x^*y^*}$	C_{z^*}	$F_{xyz}C_{z^*}$
$R_{x^*y^*z^*}$	$\varnothing^{\dagger}$	F_{xyz}

† Constraint-free limb

Table 5. Various limb output motions of the lower-mobility PMs in the spatial domain and their corresponding limb constraint wrenches.

Limb output motions of the spatial PM	Limb constraint wrenches of the spatial PM	Limb output motion of the spatial PM	Limb constraint wrenches of the spatial PM
$1T$ limb		$T_{xy}R_x$	F_zC_{yz}
T_x	$F_{yz}C_{xyz}$	$T_{x^*y^*}R_{x^*}$	$F_{z^*}C_{y^*z^*}$
T_{x^*}	$F_{y^*z^*}C_{xyz}$	$T_{x^*y^*}R_x$	$F_{z^*}C_{yz}$
$2T$ limb		$3T1R$ limb	
T_{xy}	F_zC_{xyz}	$T_{xyz}R_x$	C_{yz}
$T_{x^*y^*}$	$F_{z^*}C_{xyz}$	$1T2R$ limb	
$3T$ limb		$T_xR_{x^*y^*}$	$F_{yz}C_{z^*}$
$T_{xyz}=T_{x^*y^*z^*}$	C_{xyz}	$T_{x^*}R_{x^*y^*}$	$F_{y^*z^*}C_{z^*}$
$1R$ limb		$T_yR_{x^*y^*}$	$F_{xz}C_{z^*}$
R_x	$F_{xyz}C_{yz}$	$T_{y^*}R_{x^*y^*}$	$F_{x^*z^*}C_{z^*}$
R_{x^*}	$F_{xyz}C_{y^*z^*}$	$2T2R$ limb	
$2R$ limb		$T_{xy}R_{y^*z^*}$	$F_zC_{x^*}$
$R_{x^*y^*}$	$F_{xyz}C_{z^*}$	$T_{x^*y^*}R_{y^*z^*}$	$F_{z^*}C_{x^*}$
$3R$ limb		$3T2R$ limb	
R_{xyz}	F_{xyz}	$T_{xyz}R_{x^*y^*}$	C_{z^*}
$1T1R$ limb		$1T3R$ limb	
T_zR_z	$F_{xy}C_{xy}$	T_xR_{xyz}	F_{yz}
$T_{z^*}R_{z^*}$	$F_{x^*y^*}C_{x^*y^*}$	$T_{x^*}R_{xyz}$	$F_{y^*z^*}$
T_xR_z	$F_{yz}C_{xy}$	$2T3R$ limb	
$T_{x^*}R_{z^*}$	$F_{y^*z^*}C_{x^*y^*}$	$T_{xy}R_{xyz}$	F_z
$2T1R$ limb		$T_{x^*y^*}R_{xyz}$	F_{z^*}
$T_{xy}R_z$	F_zC_{xy}	$3T3R$ limb	
$T_{x^*y^*}R_z$	$F_{z^*}C_{xy}$	$T_{xyz}R_{xyz}$	$\varnothing$

their corresponding limb constraint wrenches.

Table 6 summarizes the desired mechanism motion twists, the corresponding mechanism constraint wrench set, and its equivalent mechanism constraint wrench sets for the planar PMs, spherical PMs, and spatial 2-DOF PMs. All members of each mechanism constraint wrench set can be constraint candidates for the constrained limbs (i.e., $\$^r_{M0i}=\$^r_{L0i}$, $\$^r_{M\infty i}=\$^r_{L\infty i}$.). For simplicity, the screws in the table are denoted as either $\boldsymbol{\$}^r_{L0s_k}=\begin{pmatrix}\hat{\boldsymbol{s}}_k & \boldsymbol{r}_k\times\hat{\boldsymbol{s}}_k\end{pmatrix}$ or $\boldsymbol{\$}^r_{L\infty s_k}=\begin{pmatrix}\boldsymbol{0} & \hat{\boldsymbol{s}}_k\end{pmatrix}$. The right superscript r of the screw represents a wrench, and each of the three letters of its right subscript from left to right represents its object type (i.e., L and M denote a limb and a mechanism, respectively), its pitch type [i.e., 0 (zero-pitch) or ∞ (infinite-pitch)], and the unit vector along the screw axis ($\hat{\boldsymbol{s}}_k$) with its subscript representing the index of the screws (k). $\boldsymbol{r}_k$ represents the position vector to the wrench axis ($\hat{\boldsymbol{s}}_k$) from the origin of the reference frame. For example, $\boldsymbol{\$}^r_{L\infty s_0}$ denotes the infinite-pitch wrench with its position vector $\boldsymbol{r}_0=\boldsymbol{0}$ and the screw axis expressed as its direction cosine $\hat{\boldsymbol{s}}_o$.

Table 6. Mechanism constraint wrenches for the planar PMs, spherical PMs, and spatial 2-DOF PMs.

Desired mechanism output motion and corresponding twists	Mechanism constraint wrench set and its equivalent mechanism constraint wrench sets
Planar T_x : $\hat{\$}_{M\infty x}$	i) $\$^r_{M0y_O}$, $\$^r_{M\infty z}$ ii) $\$^r_{M0y_1}$, $\$^r_{M0y_2}$
Planar T_{x^*} : $\hat{\$}_{M\infty x^*}$	i) $\$^r_{M0y^*_O}$, $\$^r_{M\infty z}$, ii) $\$^r_{M0y^*_1}$, $\$^r_{M0y^*_2}$
Planar R_z : $\hat{\$}_{M0z}$	i) $\$^r_{L0x_0}$, $\$^r_{L0y_0}$
Planar $T_{x^*y^*}$: $\hat{\$}_{M\infty x^*}$, $\hat{\$}_{M\infty y^*}$	i) $\$^r_{M\infty z}$
Planar T_xR_z : $\hat{\$}_{M\infty x}$, $\hat{\$}_{M0z}$	i) $\$^r_{M0y_O}$,
Planar $T_{x^*}R_z$: $\hat{\$}_{M\infty x^*}$, $\hat{\$}_{M0z}$	i) $\$^r_{M0y^*}$
Spatial $T_{x^*y^*}R_{z^*}$: $\hat{\$}_{M\infty x^*}$, $\hat{\$}_{M\infty y^*}$, $\hat{\$}_{M0z^*}$	i) $\hat{\$}^r_{M\infty x^*}$, $\hat{\$}^r_{M\infty y^*}$, $\hat{\$}^r_{M0z^*}$ ii) $\hat{\$}^r_{M0z^*_i}$, $for\ i=1,2,3$
Spherical R_z : $\hat{\$}_{M0z}$	i) $\hat{\$}^r_{M\infty x}$, $\hat{\$}^r_{M\infty y}$
Spherical $R_{x^*y^*}$: $\hat{\$}_{M0x^*}$, $\hat{\$}_{M0y^*}$	ii) $\hat{\$}^r_{M\infty z^*}=\begin{pmatrix}\boldsymbol{0} & \hat{\boldsymbol{z}}^*\end{pmatrix}$
Spherical R_{xyz} : $\hat{\$}_{M0x}$, $\hat{\$}_{M0y}$, $\hat{\$}_{M0z}$	i) $\hat{\$}^r_M=\{\varnothing\}$
Spatial T_zR_z : $\hat{\$}_{M\infty z}$, $\hat{\$}_{M0z}$	i) $\hat{\$}^r_{M0x}$, $\hat{\$}^r_{M0y}$, $\hat{\$}^r_{M\infty x}$, $\hat{\$}^r_{M\infty y}$
Spatial $T_{z^*}R_{z^*}$: $\hat{\$}_{M\infty z^*}$, $\hat{\$}_{M0z^*}$	i) $\hat{\$}^r_{M0x^*_0}$, $\hat{\$}^r_{M0y^*_0}$, $\hat{\$}^r_{L\infty 1}$ $2T_{xy}1R_z$
Spatial $\{\hat{\$}^r_{L01}\}$, : $\{\hat{\$}^r_{L\infty 1},\hat{\$}^r_{L03}\}$). $\hat{\$}_{M\infty y^*}$	i) $\hat{\$}^r_{M\infty x^*}$, $\hat{\$}^r_{M\infty y^*}$, $\hat{\$}^r_{M\infty z^*}$, $\hat{\$}^r_{M0z^*_0}$ ii) $\hat{\$}^r_{M0z^*_i}$, $for\ i=1,2$, $\hat{\$}^r_{M\infty x^*}$, $\hat{\$}^r_{M\infty y^*}$ iii) $\hat{\$}^r_{M\infty z^*}$, $\hat{\$}^r_{M\infty y^*}$, $\hat{\$}^r_{M0z^*_i}$, $for\ i=1,2$
Spatial $R_{x^*y^*}$: $\hat{\$}_{M0x^*}$, $\hat{\$}_{M0y^*}$	i) $\hat{\$}^r_{M0x^*_0}$, $\hat{\$}^r_{M0y^*_0}$, $\hat{\$}^r_{M0z^*_0}$, $\hat{\$}^r_{M\infty z^*}$ ii) $\hat{\$}^r_{M0z^*_i}$, $for\ i=1,2,3$, $\hat{\$}^r_{M\infty z^*}$

※ Constraint-free limbs ($\hat{\$}^r_L=\varnothing$) can be attached to any PM.

4. Admissible joint structures for constrained limbs

In conducting the type synthesis of the desired $mTnR$ type PMs, admissible joint structures of the various constrained limbs with respect to either the non-rotating reference frame or the rotating reference frame need to be identified. In this section, some constrained limb types, such as the C_{z^*}-, F_{z^*}-, planar F_{x^*}-, $F_{z^*}C_{z^*}$-, $F_{x^*}C_{z^*}$-, C_{yz}-, $F_{x^*y^*}$-, $F_{x^*y^*}C_{z^*}$- and $F_{z^*}C_{x^*y^*}$-type limbs, are selected since they are employed in the mechanism synthesis conducted in Sec. 5. And their admissible joint structures are investigated. In particular, type synthesis for C- and F-type limbs was similar to the one conducted in Ref. [4]. However, the results are summarized and/or categorized appropriately such that they could be employed in the target-oriented synthesis of the PMs. Other types of the constrained limbs, which are not analyzed in this section, could be analyzed by following the same procedure as addressed in this section.

4.1 C_{z^*}- type limb

The constraint wrench of the C_{z^*}-type limb imposes the pure torque constraint on the PM along the z^*-direction of the rotating reference frame of the PM, and it can be expressed as $\$^r_{L\infty 1}=\begin{pmatrix}\mathbf{0} & \hat{\boldsymbol{z}}^*\end{pmatrix}$. By applying the reciprocal conditions between the twist $\hat{\$}_{L0k}=\begin{pmatrix}\hat{\boldsymbol{s}}_k & \boldsymbol{r}_k\times\hat{\boldsymbol{s}}_k\end{pmatrix}$ of the revolute joint of the limb and the constraint wrench $\hat{\$}^r_{L\infty 1}$ of the limb, the geometric conditions can be identified, as shown in case 2 (i.e., $\hat{\boldsymbol{s}}_k$ is orthogonal to $\hat{\boldsymbol{z}}^*$). The admissible revolute joints of the limb that satisfy these conditions can be denoted as R_{x^*} and R_{y^*}. Similarly, from the reciprocal conditions between the twist $\hat{\$}_{L\infty k}=\begin{pmatrix}\mathbf{0} & \hat{\boldsymbol{s}}_k\end{pmatrix}$ of the prismatic joint of the limb and the constraint wrench $\hat{\$}^r_{L\infty z}$ of the limb, the geometric conditions for the prismatic joint can be identified, as shown in case 3 (i.e., $\hat{\boldsymbol{s}}_k$ can be arbitrary). The admissible prismatic joints of the limb that satisfy these conditions can be denoted as P_x, P_y and P_z.

The following restrictions should be imposed to secure the independence of the selected limb joints:

i) The maximum number of admissible joints is five.

ii) Those independent admissible prismatic joints (i.e., P_{x^*}, P_{y^*}, P_{z^*}) can be employed up to three times at maximum but their order is arbitrary.

iii) At least each of the two independent admissible revolute joints (i.e., R_{x^*} and R_{y^*}) should be employed but their order is arbitrary.

iv) Each of those two different types of admissible joints (i.e., R_{x^*} and R_{y^*}) can be employed repeatedly up to three times to avoid kinematic redundancy.

v) One type of admissible revolute joint should not be placed between the other type of admissible revolute joints to avoid violating the imposed limb constraint.

Following these restrictions, the admissible joint structures of the C_{z^*}-type limb can be enumerated as follows:

a) ($5R$ type): $(R_{x^*}R_{x^*}R_{x^*},R_{y^*}R_{y^*})$

b) ($4R1P$ type): $((R_{x^*},R_{x^*},R_{x^*},\{P_{x^*},P_{y^*}\}_1),R_{y^*})$, $(R_{x^*}R_{x^*}R_{x^*}R_{y^*}\{P_{x^*},P_{y^*}\}_1)$, $(R_{x^*}\{P_{x^*},P_{y^*}\}_1R_{x^*},R_{y^*}R_{y^*})$, $(R_{x^*}R_{x^*},R_{y^*}\{P_{x^*},P_{y^*}\}_1R_{y^*})$, $(R_{x^*}R_{x^*},R_{y^*}R_{y^*},\{P_{x^*},P_{y^*}\}_1)$, $(R_{x^*}R_{y^*},R_{y^*}R_{x^*},P_{z^*})$

c) ($3R2P$ type): $(R_{x^*}R_{x^*},P_{x^*},P_{y^*},R_{y^*})$, $(R_{x^*}P_{x^*}R_{x^*},P_{y^*},R_{y^*})$, $(R_{x^*}P_{y^*}R_{x^*},P_{x^*},R_{y^*})$

d) ($2R3P$ type): $(R_{x^*},P_{x^*},P_{y^*},P_{z^*},R_{y^*})$.

For simplicity, the following notations are employed in the above representations: i) A comma "," enclosed either in parenthesis or in brace implies that the order of the elements it separates is arbitrary and ii) the subscript in the brace implies that as many elements specified by the subscript can be selected from the elements in the bracket. For example, the expression $((A,\{B,C\}_1),D)$ can be expanded into (A,B,D) and (A,C,D). Furthermore, the expression (A,B,D) can be expanded into ABD, ADB, BAD, BDA, DAB, and DBA. The detailed enumerations of admissible joint structures of the C_{z^*}-type limb are detailed in Ref. [4].

4.2 F_{z^*}- and F_z- type limbs

The constraint wrench of the F_{z^*}-type limb imposes the pure-force constraint on the PM along the z^*-direction of the rotating reference frame of the PM, and it can be expressed as $\hat{\$}^r_{L01}=\begin{pmatrix}\hat{\boldsymbol{z}}^* & \boldsymbol{r}\times\hat{\boldsymbol{z}}^*\end{pmatrix}$. By applying the reciprocal conditions between the twist $\hat{\$}_{L0k}=\begin{pmatrix}\hat{\boldsymbol{s}}_k & \boldsymbol{r}_k\times\hat{\boldsymbol{s}}_k\end{pmatrix}$ of the revolute joint of limb and the constraint wrench $\hat{\$}^r_{L01}$ of the limb, the geometric conditions can be identified as case 1 of Eq. (4)

i) $\hat{\boldsymbol{s}}_k$ and $\hat{\boldsymbol{z}}^*$ are parallel

or $\hat{\boldsymbol{s}}_k$ and $\hat{\boldsymbol{z}}^*$ intersect.

The admissible revolute joints of the limb that satisfy these conditions can be denoted as R_{z^*} and R_{lz^*}. R_{z^*} is the revolute joint, the axis of which is parallel to $\hat{\boldsymbol{z}}^*$, whereas R_{lz^*} is the revolute joint, the axis of which intersects with that aligned with $\hat{\boldsymbol{z}}^*$.

Similarly, from the reciprocal conditions between $\hat{\$}_{L\infty k}=\begin{pmatrix}\mathbf{0} & \hat{\boldsymbol{s}}_k\end{pmatrix}$ and $\hat{\$}^r_{L01}$, the geometric conditions for the prismatic joints can be identified as case 2 of Eq. (5).

i) $\hat{\boldsymbol{s}}_k$ and $\hat{\boldsymbol{z}}^*$ are orthogonal : $\hat{\boldsymbol{s}}_k\cdot\hat{\boldsymbol{z}}^*=0$

The admissible prismatic joints of the limb that satisfy these conditions can be denoted as P_{x^*} and P_{y^*}.

Thus, the admissible joint structures of the F_{z^*}-limb can be formed by taking five joints out of these admissible four types of joint (i.e., $\{R_{z^*}, R_{lz^*}, P_{x^*}, P_{y^*}\}_5$, where the subscript of the bracket denotes the number of elements to sort out from the bracket. In forming the admissible structures of the F_{z^*}-type limb, the following restrictions should be imposed:

i) The maximum number of admissible joints is five.

ii) Two independent prismatic joints at maximum can be employed in the limb.

iii) Up to three revolute joints for each type of independent revolute joints can be employed.

iv) All R_{lz^*}-type joints should have the same intersection point on the z^*-axis and should be placed toward the ground prior to the other joints. Otherwise, any R_{lz^*}-type joint at cer-

tain configuration will be moved away from the z^*-axis by the motion of the other joints located toward the ground, thereby violating the condition that the joint axis intersects with the z^*-axis.

Following these restrictions, the admissible joint structure of the F_{z^*}- limb can be summarized as follows:

a) ($5R$ type):

$(R_{x^*},R_{y^*},R_{z^*})_{N_{z^*}}R_{z^*}R_{z^*}$, $(R_{x^*},R_{y^*})_{N_{z^*}}R_{z^*}R_{z^*}R_{z^*}$;

b) ($4R1P$ type): $(R_{x^*},R_{y^*},R_{z^*})_{N_{z^*}}(R_{z^*},\{P_{x^*},P_{y^*}\}_1)$, $(R_{x^*},R_{y^*})_{N_{z^*}}$, $(R_{z^*},R_{z^*},\{P_{x^*},P_{y^*}\}_1)$

c) ($3R2P$ type): $(R_{x^*},R_{y^*},R_{z^*})_{N_{z^*}}(P_{x^*},P_{y^*})$, $(R_{x^*},R_{y^*})_{N_{z^*}}(R_{z^*},P_{x^*},P_{y^*})$,

where $(R_{x^*},R_{y^*},R_{z^*})_{N_{z^*}}$ denotes three independent revolute joints whose axes intersect at a common point N_{z^*} on the z^*-axis, and their order is arbitrary. The $R_{z^*}R_{z^*}R_{z^*}$, $R_{z^*}R_{z^*}\{P_{x^*},P_{y^*}\}_1$ and $R_{z^*}P_{x^*}P_{y^*}$ joint sets above can be replaced by the other equivalent joint sets of the $F_{z^*}C_{x^*y^*}$- type limb in Sec. 4.9.

Detailed admissible joint structures corresponding to an arbitrary F- type limb was enumerated in Ref. [4]. However, all those sets in Ref. [4] are not admissible joint structures of the F_{z^*}- type limb. One more condition should be imposed on those sets in Ref. [4], that is, all the R_{lz^*}-type joints must be placed toward the ground before the other types of joints (i.e., R_{z^*}, P_{x^*} and P_{y^*}).

The F_z- type limb, which has the pure-force constraint wrench along the *z*-axis of the non-rotating reference frame, is secured only when all prismatic joint axes should be perpendicular to the *z*-axis. Moreover, all the revolute joint axes intersect at a common point on the *z*-axis. Furthermore, the revolute joint axes not parallel to the *z*-axis should be placed after all the prismatic joints of the limb, namely, (P_x,P_y) $(R_x,R_y,R_z)_{N_z}$, $R_zR_z(R_x,R_y,R_z)_{N_z}$, $(R_z,\{P_x,P_y\}_1)(R_x,R_y,R_z)_{N_z}$, $R_zR_zR_z$ $(R_x,R_y)_{N_z}$, and $R_z(P_x,P_y)(R_x,R_y)_{N_z}$. All joint axes enclosed in parentheses as $(\cdot)_{N_z}$ intersect the common point N_z on the *z*-axis.

4.3 Planar F_{x^*}- type limb

For the planar case, the constraint wrenches for the planar F_{x^*}- type limb can be written as $\hat{\$}^r_{L01}=\begin{pmatrix}\hat{\boldsymbol{x}}^* & \boldsymbol{r}\times\hat{\boldsymbol{x}}^*\end{pmatrix}$, $\hat{\$}^r_{L02}=\begin{pmatrix}\hat{\boldsymbol{z}} & \boldsymbol{0}\end{pmatrix}$, $\hat{\$}^r_{L\infty1}=\begin{pmatrix}\boldsymbol{0} & \hat{\boldsymbol{x}}\end{pmatrix}$, and $\hat{\$}^r_{L\infty2}=\begin{pmatrix}\boldsymbol{0} & \hat{\boldsymbol{y}}\end{pmatrix}$. By applying the reciprocal conditions between the twist $\hat{\$}_{L0k}=\begin{pmatrix}\hat{\boldsymbol{s}}_k & \boldsymbol{r}_k\times\hat{\boldsymbol{s}}_k\end{pmatrix}$ of the revolute joint of the limb and the constraint wrench ($\hat{\$}^r_{L0j}$, $\hat{\$}^r_{L\infty j}$, *for* $j=1,2$), the geometric conditions for the revolute joints can be identified as shown in cases 1 and 2

i) $\hat{\boldsymbol{s}}_k$ is parallel to $\hat{\boldsymbol{z}}$ and

ii) intersects with $\hat{\boldsymbol{x}}^*$, where $\hat{\boldsymbol{x}}^*$ denotes the axis of the constraint wrench $\hat{\$}^r_{L01}$.

The admissible revolute joint screw of the limb that satisfies these conditions is denoted as R_{zlx^*}.

Similarly, from cases 2 and 3, the geometric condition of the twist $\hat{\$}_{L\infty k}=\begin{pmatrix}\boldsymbol{0} & \hat{\boldsymbol{s}}_k\end{pmatrix}$ of the prismatic joint of the limb is that any prismatic joint axis should be orthogonal to the x^*- and z^*-axes, that is, $\hat{\$}_{L\infty2}=\begin{pmatrix}\boldsymbol{0} & \hat{\boldsymbol{y}}^*\end{pmatrix}$. This type of admissible prismatic joint is denoted as P_{y^*}. Thus, the candidates of the admissible joint structures of the limb can be in the form of either $(R_{zlx^*}P_{y^*})$ or ($R_{zlx^*}R_{zlx^*}$), as shown in Fig. 2.

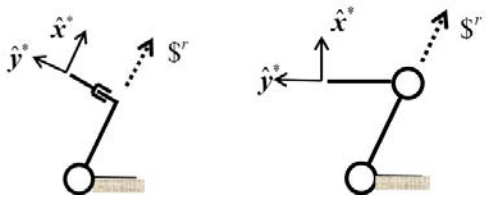

(a) (b)

Fig. 3. Admissible joint structures of the planar F_{x^*}- type limb: (a) $R_{zlx^*}P_{x^*}$-type limb; (b) $R_{zlx^*}R_{zlx^*}$-type limb.

Two limbs in Fig. 3 are different in that the orientation of the second link in Fig. 3(a) is always fixed, whereas the orientation of the second link in Fig. 3(b) can vary. Thus, when two (a)-type limbs are employed to form a four-bar linkage, the orientation of its output motion does not vary, resulting in the translational motion along the y^*-axis.

4.4 $F_{z^*}C_{z^*}$- type limb

For the constraint wrenches of the $F_{z^*}C_{z^*}$- type limb, the force constraint along the z^*-direction of the rotating reference frame of the PM and the torque constraint around the z^*-direction of the rotating reference frame of the PM can be expressed as $\hat{\$}^r_{L01}=\begin{pmatrix}\hat{\boldsymbol{z}}^* & \boldsymbol{r}\times\hat{\boldsymbol{z}}^*\end{pmatrix}$ and $\hat{\$}^r_{L\infty1}=\begin{pmatrix}\boldsymbol{0} & \hat{\boldsymbol{z}}^*\end{pmatrix}$, respectively. By applying the reciprocal conditions between the twist $\hat{\$}_{L0k}=\begin{pmatrix}\hat{\boldsymbol{s}}_k & \boldsymbol{r}_k\times\hat{\boldsymbol{s}}_k\end{pmatrix}$ of the revolute joint of the limb and the constraint wrench ($\hat{\$}^r_{L01}$, $\hat{\$}^r_{L\infty1}$), the geometric conditions for the admissible revolute joints of the limb can be identified as cases 1 and 2

i) $\hat{\boldsymbol{s}}_k$ is perpendicular to $\hat{\boldsymbol{z}}^*$

and

ii) $\hat{\boldsymbol{s}}_k$ intersects with $\hat{\boldsymbol{z}}^*$.

The admissible revolute joints that satisfy those conditions are denoted as $R_{x^*lz^*}$ and $R_{y^*lz^*}$.

Similarly, the geometric conditions for the infinite-pitch screws (or prismatic joints) are determined, as shown in cases 2 and 3,

i) any prismatic joint axis should be orthogonal to the z^*-axis.

The admissible prismatic joints that satisfy those conditions are denoted as P_{x^*} and P_{y^*}.

The admissible joint structures of the limb can be formed with four independent joints out of the four different types of joints (i.e., $R_{x^*lz^*}$, $R_{y^*lz^*}$, P_{x^*}, and P_{y^*}). In forming the admissible structures of the $F_{z^*}C_{z^*}$- type limb, the following restrictions should be considered.

i) At most, two independent prismatic joints can be employed.

ii) All revolute joints should intersect at the common point N_{z^*} on the z^*- axis.

iii) Each of the two independent revolute joints, namely, $R_{x^*Iz^*}$ and $R_{y^*Iz^*}$, can be employed three times at maximum; however, the same independent revolute joints should be adjacent. Otherwise, the condition imposed on those two independent revolute joints can be violated, that is, the axis of the following revolute joints can be moved away from the z^*- axis by the other revolute joints located toward the ground.

iv) All revolute joints should be placed toward the ground prior to any prismatic joints. Otherwise, the limb constraints with respect to the z^*-axis cannot be secured.

Thus, the admissible joint structures of the $F_{z^*}C_{z^*}$- type limb can be in the form of $(R_{x^*}R_{y^*})_{Nz^*}(R_{y^*}R_{x^*})_{Mz^*}$, $(R_{y^*}R_{x^*})_{Nz^*}(R_{x^*}R_{y^*})_{Mz^*}$ and $(R_{x^*},R_{y^*})_{Nz^*}(P_{x^*},P_{y^*})$. In particular, the joint structure $(R_{x^*}R_{y^*})_{Nz^*}(R_{y^*}R_{x^*})_{Mz^*}$ is an admissible joint structure of the $F_{z^*}C_{z^*}$- type limb because the axis of either of the two parallel revolute joints (i.e., $(R_{y^*})_{Nz^*}$ and $(R_{y^*})_{Mz^*}$) will not be changed by the rotational motion of the other revolute joints (i.e., $(R_{x^*})_{Nz^*}$ and $(R_{x^*})_{Mz^*}$) without violating the constraints imposed on them. For similar reason, the limb joint structure of $(R_{y^*}R_{x^*})_{Nz^*}(R_{x^*}R_{y^*})_{Mz^*}$ is also an admissible joint structure of the $F_{z^*}C_{z^*}$- type limb.

4.5 $F_{x^*}C_{z^*}$- *type limb*

The constraint wrenches can be expressed as $\hat{\$}^r_{L01} = \begin{pmatrix}\hat{\boldsymbol{x}}^* & \boldsymbol{r}\times\hat{\boldsymbol{x}}^*\end{pmatrix}$ and $\hat{\$}^r_{L\infty 1} = \begin{pmatrix}\boldsymbol{0} & \hat{\boldsymbol{z}}^*\end{pmatrix}$. From cases 1 and 2, geometric conditions for the zero-pitch screws ($\hat{\$}_{L0k} = \begin{pmatrix}\hat{\boldsymbol{s}}_k & \boldsymbol{r}_k\times\hat{\boldsymbol{s}}_k\end{pmatrix}$) reciprocal to all constraint wrenches can be identified as

i) either $\hat{\boldsymbol{s}}_k$ is parallel to $\hat{\boldsymbol{x}}^*$ or

ii) $\hat{\boldsymbol{s}}_k$ intersects the $\hat{\boldsymbol{x}}^*$ axis,

and

iii) $\hat{\boldsymbol{s}}_k$ is orthogonal to $\hat{\boldsymbol{z}}^*$.

The types of revolute joints satisfying both (i) and (iii) can be denoted as R_{x^*}, and the types of revolute joints satisfying both (ii) and (iii) can be denoted as $R_{x^*Ix^*}$ and $R_{y^*Ix^*}$.

Similarly, as shown in cases 2 and 3, geometric conditions for the infinite-pitch screws ($\hat{\$}_{L\infty k}$) reciprocal to all constraint wrenches are

(i) $\hat{\boldsymbol{s}}_k$ is orthogonal to $\hat{\boldsymbol{x}}^*$.

This type of admissible prismatic joints is denoted as two independent joints, P_{y^*} and P_{z^*}. Admissible joint structures of the limb can be formed with four independent joints out of those five different types of admissible joints, R_{x^*}, $R_{x^*Ix^*}$, $R_{y^*Ix^*}$, P_{y^*} and P_{z^*}. Also, the following restrictions should be taken into account.

i) Only two independent revolute joints could be used.

ii) Those two independent revolute joints should intersect at the common point N_{x^*} on the $\hat{\boldsymbol{x}}^*$- axis. Otherwise, conditions imposed on the two revolute joints are violated.

iii) Two independent prismatic joints should be employed before the revolute joints to secure the motion with respect to the axes of the non-rotating reference frame.

Note that when $\boldsymbol{r}=\boldsymbol{0}$, the axis of the zero-pitch constraint wrench $\hat{\$}^r_{L01} = \begin{pmatrix}\hat{\boldsymbol{x}}^* & \boldsymbol{r}\times\hat{\boldsymbol{x}}^*\end{pmatrix}$ coincides with the $\hat{\boldsymbol{x}}^*$ axis of the rotating reference frame. In that case, R_{x^*} and $R_{x^*Ix^*}$ are identical. Thus, two admissible joint structures are feasible, $R_{x^*Ix^*}R_{y^*Ix^*}P_{z^*}P_{y^*}$ and $R_{x^*Ix^*}R_{y^*Ix^*}P_{y^*}P_{z^*}$. Fig. 4 shows the case whose joint structure is $R_{x^*Ix^*}R_{y^*Ix^*}P_{z^*}P_{y^*}$, where the first revolute joint is aligned with the $\hat{\boldsymbol{x}}^*$ axis and the axis of the second revolute joint passes through the $\hat{\boldsymbol{x}}^*$ axis. In fact, the axis of the constraint wrenches imposed on the limb passes through the intersection point between those two revolute joint axes.

Fig. 4. The admissible joint structures of the $F_{x^*}C_{z^*}$ – limb: $R_{x^*Ix^*}R_{y^*Ix^*}P_{z^*}P_{y^*}$ type limb.

4.6 C_{yz}- *type limb*

The constraint wrenches can be identified as $\hat{\$}^r_{L\infty 1} = \begin{pmatrix}\boldsymbol{0} & \hat{\boldsymbol{y}}\end{pmatrix}$ and $\hat{\$}^r_{L\infty 2} = \begin{pmatrix}\boldsymbol{0} & \hat{\boldsymbol{z}}\end{pmatrix}$. By applying the results shown in cases 2 and 3, the geometric conditions for the admissible revolute joints of the C_{yz}- type limb can be identified as follows: $\hat{\boldsymbol{s}}_k$ is perpendicular to $\hat{\boldsymbol{y}}_k$ and $\hat{\boldsymbol{z}}_k$, where the revolute joint screw is expressed as $\$_{L01} = \begin{pmatrix}\hat{\boldsymbol{s}} & \boldsymbol{r}\times\hat{\boldsymbol{s}}\end{pmatrix}$. This type of revolute joints is denoted as R_x. No geometric condition is imposed on the prismatic joints by the C_{yz}- type limb. The type of admissible prismatic joints is denoted as P_x, P_y and P_z.

The admissible joint structures of the limb can be formed by combining the above two different types of joints (i.e., R_x, P_x, P_y and P_z). However, the following restrictions should be considered.

i) Four joints among those four admissible joint types should be selected.

ii) The revolute joint can be employed three times at most.

iii) Three independent prismatic joints can be used at most.

The x- axis of the C_{yz}- type limb always remains fixed even when the PM is in motion. Thus, the admissible joint structure can be identified as (P_x,P_y,P_z,R_x), $(\{P_y,P_z\}_1, (P_x,R_x,R_x))$ and (P_x,R_x,R_x,R_x). Various admissible joint structures can be identified by arbitrarily changing the order of the elements in the parentheses.

4.7 $F_{x^*y^*}$- *limb*

The constraint wrenches of the $F_{x^*y^*}$- limb can be expressed as $\hat{\$}^r_{L01} = \begin{pmatrix}\hat{\boldsymbol{x}}^* & \hat{\boldsymbol{r}}_1\times\hat{\boldsymbol{x}}^*\end{pmatrix}$ and $\hat{\$}^r_{L02} = \begin{pmatrix}\hat{\boldsymbol{y}}^* & \hat{\boldsymbol{r}}_2\times\hat{\boldsymbol{y}}^*\end{pmatrix}$. By applying the results shown in case 1, geometric conditions for the zero-pitch twists ($\hat{\$}_{L0k} = \begin{pmatrix}\hat{\boldsymbol{s}}_k & \boldsymbol{r}_k\times\hat{\boldsymbol{s}}_k\end{pmatrix}$) can be identified as follows

i) either $\hat{\boldsymbol{s}}_k$ is parallel to $\hat{\boldsymbol{x}}^*$ or

ii) $\hat{\boldsymbol{s}}_k$ intersects $\hat{\boldsymbol{x}}^*$,

and

iii) either $\hat{\boldsymbol{s}}_k$ is parallel to $\hat{\boldsymbol{y}}^*$ or

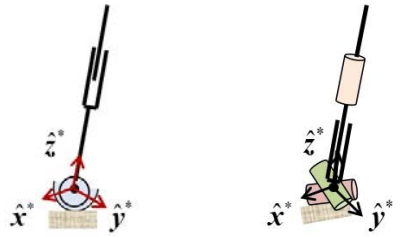

(a) (b)

Fig. 5. The admissible joint structures of the $F_{x^*y^*}$- limb: (a) $(R_{x^*}, R_{y^*}, R_{z^*})_O P_{z^*}$ type limb; (b) $(R_{x^*}, R_{y^*})_O P_{z^*}(R_{z^*})_O$ type limb.

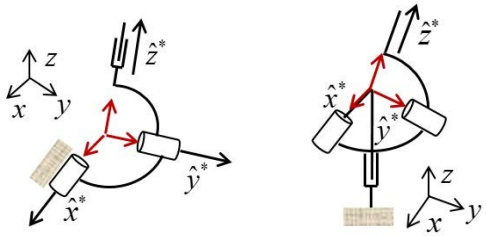

(a) (b)

Fig. 6. The $F_{x^*y^*}C_{z^*}$- limb and the $F_{xy}C_{z^*}$- limb: (a) The $(R_{x^*ly^*}R_{y^*lx^*})_O P_{z^*}$ type limb; (b) $P_z(R_{x^*ly^*}R_{y^*lx^*})_O$ type limb.

iv) $\hat{\boldsymbol{s}}_k$ intersects $\hat{\boldsymbol{y}}^*$.

Thus, there is no revolute joint type satisfying (i) and (iii). Two different types of revolute joints can be identified from (i) and (iv) and from (ii) and (iii), and from (ii) and (iv), and they are denoted as $R_{x^*y^*}$ and R_{lO}. Here, $R_{x^*y^*}$ and R_{lO} denotes the revolute joint whose axis lies on the x^*-y^* plane and the revolute joint whose axis passes through the origin of the rotating reference frame, respectively. Similarly, the geometric conditions of the prismatic joints require that any prismatic joint axis should be orthogonal to the x^*-y^* plane. This type joint is denoted as P_{z^*}.

Thus, the admissible joint structures of the $F_{x^*y^*}$- limb could be formed with four independent joints out of three different types of joints: $R_{x^*y^*}$, R_{lO} and P_{z^*}. Thus, there is no admissible joint structures satisfying such condition except cases of employing three independent R_{lO}'s as $(R_{x^*}, R_{y^*}, R_{z^*})_O P_{z^*}$ and $(R_{x^*}, R_{y^*})_O P_{z^*}(R_{z^*})_O$. Figs. 5(a) and (b) show these two limb structures, respectively. Remark that each axis of the desired constraints imposed on the limb passes through the origin of the rotating reference frames located at the centers of the spherical joint and the universal joint, respectively as shown in Fig. 5.

By following the similar reasoning, the admissible joint structures for the F_{xy}- limb are identified as $P_z(R_x R_y R_z)_O$ and $R_z P_z(R_x R_y)_O$, respectively.

4.8 The $F_{x^*y^*}C_{z^*}$- limb

The constraint wrenches of the $F_{x^*y^*}C_{z^*}$- limb can be written as $\hat{\$}^r_{L01} = \begin{pmatrix} \hat{\boldsymbol{x}}^* & \boldsymbol{r}_1 \times \hat{\boldsymbol{x}}^* \end{pmatrix}$, $\hat{\$}^r_{L02} = \begin{pmatrix} \hat{\boldsymbol{y}}^* & \boldsymbol{r}_2 \times \hat{\boldsymbol{y}}^* \end{pmatrix}$, and $\hat{\$}^r_{L\infty 1} = \begin{pmatrix} \boldsymbol{0} & \hat{\boldsymbol{z}}^* \end{pmatrix}$. By applying the results shown in cases 1 and 2, the geometric conditions for the admissible revolute joints of the $F_{x^*y^*}C_{z^*}$- type limb can be identified as follows.

i) $\hat{\boldsymbol{s}}_j$ either is parallel to $\hat{\boldsymbol{x}}^*$ or intersects the $\hat{\boldsymbol{x}}^*$ axis,

(ii) $\hat{\boldsymbol{s}}_j$ either is parallel to $\hat{\boldsymbol{y}}^*$ or intersects the $\hat{\boldsymbol{y}}^*$ axis, and

iii) $\hat{\boldsymbol{s}}_j$ is orthogonal to $\hat{\boldsymbol{z}}^*$.

These conditions can be summarized as (a) $\hat{\boldsymbol{s}}_j$ is parallel to $\hat{\boldsymbol{x}}^*$ and intersects the $\hat{\boldsymbol{y}}^*$ axis, (b) $\hat{\boldsymbol{s}}_j$ is parallel to $\hat{\boldsymbol{y}}^*$ or intersects the $\hat{\boldsymbol{x}}^*$ axis, and (c) $\hat{\boldsymbol{s}}_j$ should intersect both the $\hat{\boldsymbol{x}}^*$ axis and the $\hat{\boldsymbol{y}}^*$ axis. The types of the revolute joint satisfying the condition (a), (b) and (c) are denoted as $R_{x^*ly^*}$, $R_{y^*lx^*}$ and $R_{lx^*ly^*}$, respectively. Similarly, the geometric condition of the prismatic joints requires that any prismatic joint axis should be orthogonal to the x^*-y^* plane. This type joint is denoted as P_{z^*}.

Thus, the admissible joint structures of the $F_{x^*y^*}C_{z^*}$- limb could be formed with three independent joints out of three different types of resolute joints ($R_{x^*ly^*}$, $R_{y^*lx^*}$, $R_{lx^*ly^*}$) and one prismatic joint (P_{z^*}). Since those three different types of revolute joints lie on the same plane, only two independent revolute joints out of those three could be employed to form the admissible limb. Further, since any those two revolute joints intersect, the joint structures of the $F_{x^*y^*}C_{z^*}$- limb can be identified as $(\{(R_{x^*ly^*}, R_{y^*lx^*}, R_{lx^*ly^*})_O\}_2 P_{z^*})$. Similarly, admissible joint structure of the $F_{xy}C_{z^*}$ – limb can be identified as $P_z\{(R_{x^*ly^*}, R_{y^*lx^*}, R_{lx^*ly^*})_O\}_2$. Figs. 6(a) and (b) show examples of such two different constrained limb joint structures; a $(R_{x^*ly^*}R_{y^*lx^*})_O P_{z^*}$ type limb and a type limb, respectively.

4.9 $F_{z^*}C_{x^*y^*}$- type limb

Note that the joint structures of the $F_{z^*}C_{x^*y^*}$- type limb can be obtained by replacing the subscript z by z^* in the ones of the F_zC_{xy}- type limb. Thus, the joint structure of the F_zC_{xy}- type limb is analyzed.

The constraint wrenches of the F_zC_{xy}- type limb can be expressed as $\hat{\$}^r_{L\infty 1} = \begin{pmatrix} \boldsymbol{0} & \hat{\boldsymbol{x}} \end{pmatrix}$, $\hat{\$}^r_{L\infty 2} = \begin{pmatrix} \boldsymbol{0} & \hat{\boldsymbol{y}} \end{pmatrix}$ and $\hat{\$}^r_{L01} = \begin{pmatrix} \hat{\boldsymbol{z}} & \boldsymbol{r} \times \hat{\boldsymbol{z}} \end{pmatrix}$. The zero-pitch twist ($\hat{\$}_{L0j} = \begin{pmatrix} \hat{\boldsymbol{s}}_j & \boldsymbol{r}_j \times \hat{\boldsymbol{s}}_j \end{pmatrix}$) reciprocal to all three constraint wrenches should satisfy the following condition.

i) $\hat{\boldsymbol{s}}_j$ either is parallel to $\hat{\boldsymbol{z}}$ or intersects the $\hat{\boldsymbol{z}}$ axis and

ii) is perpendicular to both $\hat{\boldsymbol{x}}$ and $\hat{\boldsymbol{y}}$.

This type of the revolute joint satisfying those conditions is denoted as R_z. Similarly, the infinite-pitch twists reciprocal to those three constraint wrenches can be identified as:

i) $\hat{\$}_{L\infty 1} = \begin{pmatrix} \boldsymbol{0} & \hat{\boldsymbol{x}} \end{pmatrix}$ and $\hat{\$}_{L\infty 2} = \begin{pmatrix} \boldsymbol{0} & \hat{\boldsymbol{y}} \end{pmatrix}$.

These prismatic joints are denoted as two independent ones (i.e., P_x and P_y). Thus, the admissible joint structures of the limb can be formed with three independent joints out of the two different joint types, namely, R_z, P_x and P_y.

As previously discussed, these constraints of the F_zC_{xy}- type limb allow the planar $2T_{xy}1R_z$-type 3-DOF motion. Thus, the joint structures of the F_zC_{xy}- type limb (or the planar $2T_{xy}1R_z$ -type 3-DOF limb) can be identified as $R_zR_zR_z$, R_zR_zP R_zPR_z, PR_zR_z, R_zPP, PR_zP, and

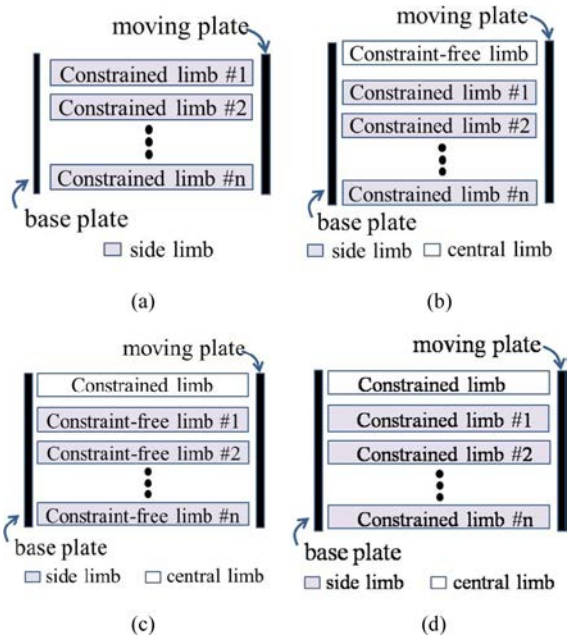

Fig. 7. PM structures: (a) With several side limbs; (b) with a constraint-free central limb and several constrained side limbs; (c) with a constrained central limb and several constraint-free side limbs; (d) with a constrained central limb and several constrained side limbs.

PPR_z, where P could be either P_x or P_y and two prismatic joints are selected as independent.

5. Type synthesis of the lower-mobility PMs

As the first part of this section, the architecture of the symmetric and asymmetric PMs is briefly discussed. Then the task-oriented type syntheses of the lower-mobility PMs are conducted by following the procedure suggested in Sec. 2.2. For simplicity, three different types of PMs including planar $1T_{y^*}$ -type 1-DOF PM, spatial $2T_{x^*y^*}$ -type PM, and spatial $1T_{z^*}2R_{x^*y^*}$ -type PM are selected as exemplary PMs.

5.1 Architecture of the symmetric and asymmetric PM

Fig. 7(a) shows the typical PM structure with symmetric limbs. Conversely, all constrained limbs for the asymmetric PMs are not identical. Various types of the asymmetric PMs exist. However, for simplicity, only several asymmetric PM structures with a central limb and several side limbs are addressed as exemplary cases.

Fig. 7(b) shows the structure with a central constraint-free limb and several constrained side limbs, Fig. 7(c) shows the structure with constrained central limb and several constraint-free side limbs, and Fig. 7(d) shows the structure with a constrained central limb and three constraint-free side limbs. Other various forms of the asymmetric PMs can also be formed by adding several constraint-free limbs to the asymmetric PMs. The desired role of the constraint-free limbs, if any, can be either to reinforce the stiffness or provide active inputs.

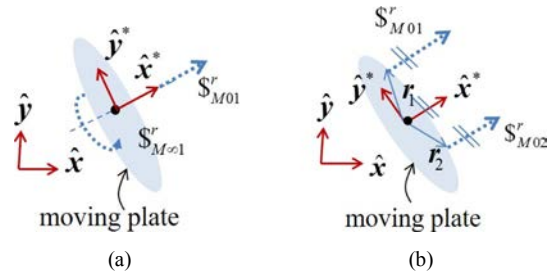

Fig. 8. Equivalent mechanism constraints for the $1T_{y^*}$ -type 1-DOF PM: (a) F_{x^*} - and C_z -type constraints; (b) two F_{x^*} -type constraints.

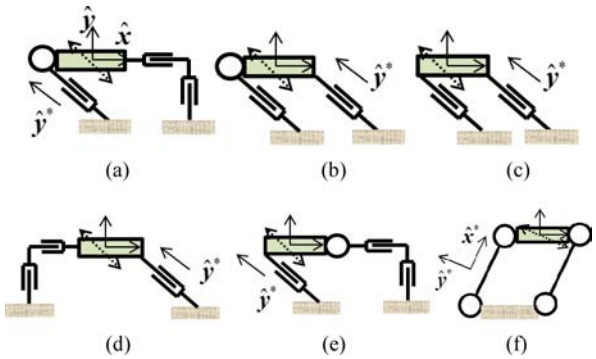

Fig. 9. Planar $1T_{y^*}$ -type 1-DOF PMs with two constrained limbs: (a) ($\{\$^r_{L01}\}$, $\{\$^r_{L\infty 1}\}$); (b) ($\{\$^r_{L01}\}$, $\{\$^r_{L01},\$^r_{L\infty 1}\}$); (c) ($\{\$^r_{L01},\$^r_{L\infty 1}\}$, $\{\$^r_{L01},\$^r_{L\infty 1}\}$); (d) ($\{\$^r_{L\infty 1}\}$, $\{\$^r_{L01},\$^r_{L\infty 1}\}$); (e) ($\{\$^r_{L01},\$^r_{L\infty 1}\}$, $\{\varnothing\}$); (f) ($\{\$^r_{L01}\}$, $\{\$^r_{L01}\}$).

5.2 Planar $1T_{y^*}$ -type 1-DOF PM

The desired motion screw of the $1T_{y^*}$ -type 1- DOF PM is $\hat{\$}_{M\infty 1}=\begin{pmatrix}\mathbf{0} & \hat{\boldsymbol{y}}^*\end{pmatrix}$. Two constraint wrenches imposed on the planar PM, which are reciprocal to the desired motion screw, can be identified as $\hat{\$}^r_{M01}=\begin{pmatrix}\hat{\boldsymbol{x}}^* & \mathbf{0}\end{pmatrix}$ and $\hat{\$}^r_{M\infty 1}=\begin{pmatrix}\mathbf{0} & \hat{\boldsymbol{z}}\end{pmatrix}$, as shown in Fig. 8(a). These two constraint wrenches can be replaced by two pure-force constraint wrenches, as shown in Fig. 8(b). The two mechanism constraints shown in Fig. 8(b) are identical, that is, $\hat{\$}^r_{M0i}=\begin{pmatrix}\hat{\boldsymbol{x}}^* & \boldsymbol{r}_i\times\hat{\boldsymbol{x}}^*\end{pmatrix}$, *for* $i=1,2$. Only one feasible PM structure has two constrained limbs with one of $\hat{\$}^r_{L0i}$'s, where $\hat{\$}^r_{L0i}=\hat{\$}^r_{M0i}$. Conversely, the mechanism constraints shown in Fig. 8(a) has two different constraints, which are expressed as $\hat{\$}^r_{M01}=\begin{pmatrix}\hat{\boldsymbol{x}}^* & \boldsymbol{r}_1\times\hat{\boldsymbol{x}}^*\end{pmatrix}$ and $\hat{\$}^r_{M\infty 1}=\begin{pmatrix}\mathbf{0} & \hat{\boldsymbol{z}}\end{pmatrix}$. Thus, two different limb constraints are considered in the following synthesis of the 1-DOF planar PMs. In this analysis, the limb constraint wrenches and the mechanism constraint wrenches are the same as $\hat{\$}^r_{L01}=\hat{\$}^r_{M01}$ and $\hat{\$}^r_{L\infty 1}=\hat{\$}^r_{M\infty 1}$.

Four different types of constrained limbs can be employed. These constrained limbs are characterized by their constraint wrenches (i.e., $\{\$^r_{L01}\}$, $\{\$^r_{L\infty 1}\}$, $\{\$^r_{L01},\$^r_{L\infty 1}\}$, and $\{\varnothing\}$, where $\{\varnothing\}$ implies a constraint-free limb). Thus, admissible constrained limb sets of the planar 1-DOF PMs with two limbs

can be formed as ($\{\$^r_{L01}\}$, $\{\$^r_{L01}\}$), ($\{\$^r_{L01}\}$, $\{\$^r_{L\infty1}\}$), ($\{\$^r_{L01},\$^r_{L\infty1}\}$, $\{\$^r_{L01}\}$), ($\{\$^r_{L01},\$^r_{L\infty1}\}$, $\{\$^r_{L\infty1}\}$), ($\{\$^r_{L01},\$^r_{L\infty1}\}$, $\{\$^r_{L01},\$^r_{L\infty1}\}$) and ($\{\$^r_{L01},\$^r_{L\infty1}\}$, $\{\varnothing\}$). Fig. 9 shows six different types of PMs with the corresponding limb structures. The planar parallelogram in Fig. 9(f) is an example of the symmetric PM, which has a limb constraint set ($\{\$^r_{L01}\}$, $\{\$^r_{L01}\}$), as shown in Fig. 8(b), and has two R_zR_z -type limbs. Any planar F_x- or C_z- type limb can also be used to form a $1T_{y^*}$ PM.

5.3 Spatial $2T_{x^*y^*}$ *-type 2-DOF PM*

Assume that the desired motion screws of the $2T_{x^*y^*}$ -type 2-DOF PM are $\hat{\$}_{M\infty1}=\begin{pmatrix}\mathbf{0} & \hat{\boldsymbol{x}}^*\end{pmatrix}$ and $\hat{\$}_{M\infty2}=\begin{pmatrix}\mathbf{0} & \hat{\boldsymbol{y}}^*\end{pmatrix}$. The four constraint wrenches imposed on the PM, which are reciprocal to the desired motion screws, can be identified as $\hat{\$}^r_{M\infty1}=\begin{pmatrix}\mathbf{0} & \hat{\boldsymbol{x}}^*\end{pmatrix}$, $\hat{\$}^r_{M\infty2}=\begin{pmatrix}\mathbf{0} & \hat{\boldsymbol{y}}^*\end{pmatrix}$, $\hat{\$}^r_{M\infty3}=\begin{pmatrix}\mathbf{0} & \hat{\boldsymbol{z}}^*\end{pmatrix}$, and $\hat{\$}^r_{M01}=\begin{pmatrix}\hat{\boldsymbol{z}}^* & \boldsymbol{r}\times\hat{\boldsymbol{z}}^*\end{pmatrix}$. It should be noted that three infinite-pitch constraint wrenches ($\hat{\$}^r_{M\infty1}$, $\hat{\$}^r_{M\infty2}$, and $\hat{\$}^r_{M\infty3}$) could be replaced by any three independent infinite-pitch constraint wrenches and that $\boldsymbol{r}$ in $\hat{\$}^r_{M01}$ is arbitrary.

Fig. 10(a) shows those four mechanism constraints. Figs. 10(b) and 10(c) show their equivalent mechanism constraint sets. As shown in Fig. 10, all admissible constrained limbs could be identified as follows: F_{z^*}- , C_{x^*}- , C_{y^*}- , C_{z^*}- , $C_{x^*y^*}$- , $C_{x^*z^*}$- , $C_{y^*z^*}$- , $F_{z^*}C_{x^*}$- , $F_{z^*}C_{y^*}$- , $F_{z^*}C_{z^*}$- , $F_{z^*}C_{x^*y^*}$- , $F_{z^*}C_{x^*z^*}$- , $F_{z^*}C_{y^*z^*}$- , $C_{x^*y^*z^*}$- and $F_{z^*}C_{x^*y^*z^*}$- limbs.

In particular, the structures of the non-over-constrained PMs could be formed by assigning the constraints in one of Figs. 10(a)-(c) to each of three limbs of the PM without duplication. For example, for the non-over-constrained PM with constraints as in Fig. 10(a), its limb constraints can be selected as follows: one limb has two constraints out of six different constraint sets (i.e., $\{\hat{\$}^r_{L\infty1},\hat{\$}^r_{L01}\}$, $\{\hat{\$}^r_{L\infty2},\hat{\$}^r_{L01}\}$, $\{\hat{\$}^r_{L\infty3},\hat{\$}^r_{L01}\}$, $\{\hat{\$}^r_{L\infty1},\hat{\$}^r_{L\infty2}\}$, $\{\hat{\$}^r_{L\infty1},\hat{\$}^r_{L\infty3}\}$, and $\{\hat{\$}^r_{L\infty2},\hat{\$}^r_{L\infty3}\}$), and each of the other two limbs have one constraint out of remaining ones from all four different constraints (i.e., $\{\hat{\$}^r_{L\infty1}\}$, $\{\hat{\$}^r_{L\infty2}\}$, $\{\hat{\$}^r_{L\infty2}\}$, $\{\hat{\$}^r_{L01}\}$, without duplication. In the above, it is assumed, without loss of generality, that $\hat{\$}^r_{L\infty i}=\hat{\$}^r_{M\infty i}$, *for* $i=1,2,3,$ and $\hat{\$}^r_{L01}=\hat{\$}^r_{M01}$. Note that the reference frames of all constrained limbs are the same as the one of the PM. Fig. 11(a) shows an example of the non-over-constrained PM with the C_{x^*}- limb, the C_{y^*}- limbs, and the $F_{z^*}C_{z^*}$- limb.

Also, the structures of the non-over-constrained PM with constraints as in Fig. 10(b), can be formed with two F_{z^*}- limbs and one $F_{z^*}C_{z^*}$- limb. Note that the force constraint wrench axes of those three limbs must be parallel one another. Fig. 11(b) shows such an example PM having two F_{z^*}- type limbs whose joint structure are $(R_{x^*}R_{y^*})_{Nz^*}(R_{x^*}R_{y^*}R_{z^*})_{Mz^*}$ and one $F_{z^*}C_{z^*}$- type limb whose joint structure is $(R_{x^*}R_{y^*})_{Nz^*}(R_{y^*}R_{x^*})_{Mz^*}$. Similarly, the structures of the non-over-constrained PM with constraints as in Fig. 10(c), could be formed with the proper combinations of the following admissible limbs: F_{z^*}- , C_{x^*}- , C_{y^*}- $F_{z^*}C_{z^*}$- , $F_{z^*}C_{x^*}$- , $F_{z^*}C_{y^*}$- , $C_{x^*}C_{z^*}$- , $C_{y^*}C_{z^*}$- limbs. Fig. 11(c) shows an example of the asymmetric non-over-constrained PM which employs three

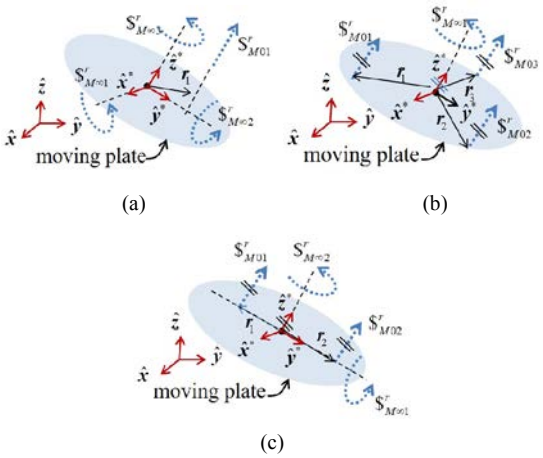

(a) (b) (c)

Fig. 10. Equivalent mechanism constraints for the $2T_{x^*y^*}$ -type 2-DOF PM: (a) Type-A mechanism constraints; (b) type-B mechanism constraints; (c) type-C mechanism constraints.

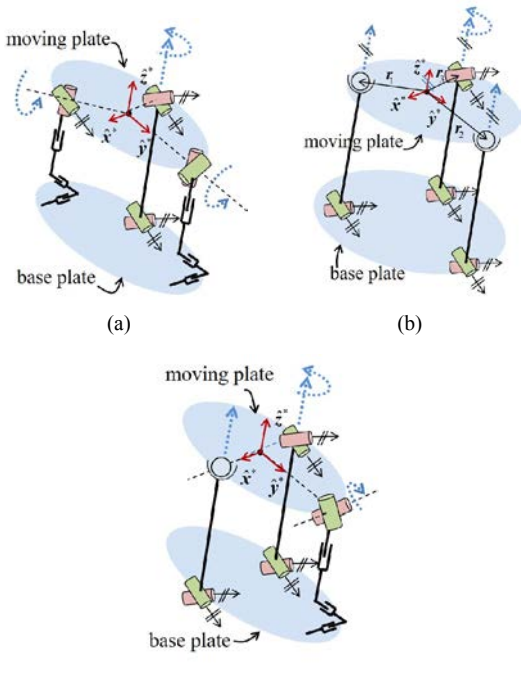

(a) (b) (c)

Fig. 11. Examples of the $2T_{x^*y^*}$ -type 2-DOF asymmetric and non-over-constrained PMs: (a) With type-A mechanism constraints; (b) with type-B mechanism constraints; (c) with type-C mechanism constraints.

different limbs: one F_{z^*}- limb, one C_{x^*}- limb, and one $F_{z^*}C_{z^*}$- limb.

The structures of the over-constrained PMs based on the constraint wrenches shown in Figs. 10(a) and (b) are examined in detail. The other case (Fig. 10(c)) is not discussed because it can be treated in a similar manner. In Fig. 10(a), the four independent constraints imposed on the PM are expressed as $\hat{\$}^r_{L\infty1}$, $\hat{\$}^r_{L\infty2}$, $\hat{\$}^r_{L\infty3}$ and $\hat{\$}^r_{L01}$. Various over-constrained PMs can be formed by the overlapped distribution of these four constraints to the limbs. The PM structures are valid

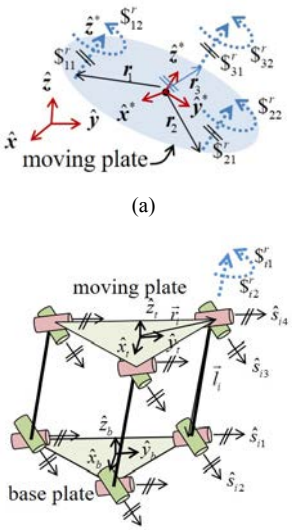

Fig. 12. Over-constrained PM: (a) Limb constraints; (b) spatial $2T_{x^*y^*}$ parallelogram.

when all these four different constraints are included in one of the selected limbs. Candidates of the limb constraints for the over-constrained PMs can be expressed as $\{\hat{\$}^r_{L01}\}$, $\{\hat{\$}^r_{L\infty i}\}$, $\{\hat{\$}^r_{L\infty i},\hat{\$}^r_{L\infty j}\}$, $\{\hat{\$}^r_{L\infty i},\hat{\$}^r_{M01}\}$, $\{\hat{\$}^r_{L\infty 1},\hat{\$}^r_{L\infty 2},\hat{\$}^r_{L\infty 3}\}$, $\{\hat{\$}^r_{L\infty i},\hat{\$}^r_{L\infty j},\hat{\$}^r_{M01}\}$, and $\{\hat{\$}^r_{L\infty 1},\hat{\$}^r_{L\infty 2},\hat{\$}^r_{L\infty 3},\hat{\$}^r_{L01}\}$, *for* $i=1,2,3$, $j=i+1,3$ $(i\neq 3)$. Note that the constrained limb with $\{\hat{\$}^r_{L\infty 1},\hat{\$}^r_{L\infty 2},\hat{\$}^r_{L\infty 3},\hat{\$}^r_{L01}\}$ has a planar translational 2-DOF motion and thus is not adequate for the limb of the spatial $2T_{x^*y^*}$ -type 2-DOF PM.

Four independent constraints imposed on the PM in Fig. 10(b) can be expressed as $\hat{\$}^r_{L\infty 1}=\begin{pmatrix}\mathbf{0} & \hat{\boldsymbol{z}}^*\end{pmatrix}$ and $\hat{\$}^r_{L0i}=\begin{pmatrix}\hat{\boldsymbol{z}}^* & \boldsymbol{r}_i\times\hat{\boldsymbol{z}}^*\end{pmatrix}$, *for* $i=1,2,3$. Various over-constrained PMs can be formed by the overlapped distribution of these four constraints to the limbs. Each limb of the over-constrained PM has one of the constraint sets (i.e., $\{\hat{\$}^r_{L\infty 1}\}$, $\{\hat{\$}^r_{L01}\}$, and $\{\hat{\$}^r_{L\infty 1},\hat{\$}^r_{L01}\}$). Fig. 12(a)) shows an over-constrained PM where each of three limbs has the same constraints, that is, each limb of the PM has the $F_{z^*}C_{z^*}$- limb, i.e., one zero-pitch constraint wrench and one infinite-pitch constraint wrench $\{\hat{\$}^r_{L\infty 1},\hat{\$}^r_{L01}\}$. The admissible joint structure of this type of limb is discussed in Sec. 4.4. The PM in Fig. 12(b) is a 2-DOF spatial parallelogram with three identical $(R_{x^*}R_{y^*})_{Nz^*}(R_{y^*}R_{x^*})_{Mz^*}$ -type limbs.

5.4 The $1T_{z^*}2R_{x^*y^*}$ *type 3-DOF PM*

The desired output motion screws of the $1T_{z^*}2R_{x^*y^*}$ type 3-DOF PM are selected as $\hat{\$}_{M\infty 1}=\begin{pmatrix}\mathbf{0} & \hat{\boldsymbol{z}}^*\end{pmatrix}$, $\hat{\$}_{M01}=\begin{pmatrix}\hat{\boldsymbol{x}}^* & \mathbf{0}\end{pmatrix}$, $\hat{\$}_{M02}=\begin{pmatrix}\hat{\boldsymbol{y}}^* & \mathbf{0}\end{pmatrix}$. Using reciprocal conditions, the simplified forms of constraint wrenches of the PM can be identified as $\hat{\$}^r_{M01}=\begin{pmatrix}\hat{\boldsymbol{x}}^* & \boldsymbol{r}_1\times\hat{\boldsymbol{x}}^*\end{pmatrix}$, $\hat{\$}^r_{M02}=\begin{pmatrix}\hat{\boldsymbol{y}}^* & \boldsymbol{r}_2\times\hat{\boldsymbol{y}}^*\end{pmatrix}$, and $\hat{\$}^r_{M\infty 1}=\begin{pmatrix}\mathbf{0} & \hat{\boldsymbol{z}}^*\end{pmatrix}$. Note that $\hat{\$}^r_{M01}$ and $\hat{\$}^r_{M02}$ can be replaced by any two independent constraint wrenches whose axes lie on the plane perpendicular to the $\hat{z}^*$ axis. Fig. 13(a) shows the mechanism constraints where both $\boldsymbol{r}_1$ in $\hat{\$}^r_{M01}$ and $\boldsymbol{r}_2$ in $\hat{\$}^r_{M02}$ are set as null vectors, without loss of generality. Fig. 13(b) shows the

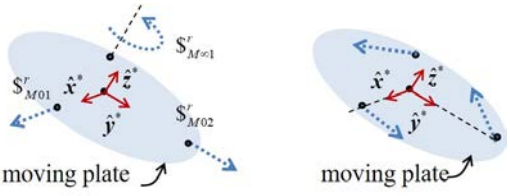

Fig. 13. Equivalent mechanism constraints for the $1T_{z^*}2R_{x^*y^*}$ -type spatial 3-DOF PM: (a) Mechanism constraints; (b) equivalent mechanism constraints.

equivalent mechanism constraints to ones in Fig. 13(a), i.e., three zero-pitch constraint wrenches ($\hat{\$}^r_{M01}$, $\hat{\$}^r_{M02}$ and $\hat{\$}^r_{M03}$). Note that these constraint wrenches are expressed as $\hat{\$}^r_{M0i}=\begin{pmatrix}\hat{\boldsymbol{s}}_i & \boldsymbol{r}_i\times\hat{\boldsymbol{s}}_i\end{pmatrix}$, *for* $i=1,2,3$, where $\boldsymbol{r}_i\times\hat{\boldsymbol{s}}_i$ is parallel to $\hat{\boldsymbol{z}}^*$.

In fact, those constraint wrenches of the PM can be distributed to limbs in several different ways. Noting that there are three independent limb constraints in Fig. 13, five different types of limb constraint wrenches can be identified as: $\{\hat{\$}^r_{L01}\}$, $\{\hat{\$}^r_{L\infty 1}\}$, $\{\hat{\$}^r_{L01},\hat{\$}^r_{L02}\}$, $\{\hat{\$}^r_{L01},\hat{\$}^r_{L\infty 1}\}$, and $\{\hat{\$}^r_{L01},\hat{\$}^r_{L02},\hat{\$}^r_{L\infty 1}\}$, where $\hat{\$}^r_{M0i}=\hat{\$}^r_{L0i}$, $\hat{\$}^r_{M\infty 1}=\hat{\$}^r_{L\infty 1}$, for $i=1,2,3$. Note that these correspond to the F_{x^*}- , the C_{z^*}- , the $F_{x^*y^*}$- , the $F_{x^*}C_{z^*}$- and $F_{x^*y^*}C_{z^*}$- limbs, respectively.

The admissible joint structures of those five different constrained limbs are already discussed in Sec. 4 and thus are not repeated here. With those five different types of constrained limbs, various forms of the PMs, whether symmetric or asymmetric, could be constructed by following the procedure as discussed in Sec. 2.2. Again it is assumed that the PMs with three limbs are considered.

For simplicity, in forming the exemplary PMs, one simple joint structure for each of five constrained limbs are employed: i) the $(R_xR_yR_z)_OP_{z^*}P_{x^*}$ type limb for the F_{x^*}- limb, ii) the $(R_{x^*}R_{y^*})_{Nz^*}P_{z^*}(R_{y^*}R_{x^*})_{Mz^*}$ type limb for the C_{z^*}- limb, and iii) the $(R_xR_yR_z)_OP_{z^*}$ type limb for the $F_{x^*y^*}$- limb, the $(R_{x^*}R_{y^*})_OP_{z^*}P_{y^*}$ type limb for the $F_{x^*}C_{z^*}$- limb, and the $(R_{x^*}R_{y^*})_OP_{z^*}$ type limb for the $F_{x^*y^*}C_{z^*}$- limb.

Figs. 14(a) and (b) show two non-over-constrained structures of the PM. Figs. 14(c)-(e) show three over-constrained structures of the PMs. Note that the base points of three limbs of the PM in Fig. 14(e) must be identical. Fig. 14(f) shows another version of Fig. 14(a). The PM employs the same joint structures of the constrained limbs but the spherical joints, which are replaced by three revolute joints, are located at the center of the universal joint of the C_{z^*}- limb.

Only a few exemplary PMs are illustrated in this work, However, any other admissible joint structures as shown in Sec. 4 could be employed to form other huge number of structures of the PMs satisfying the desired output motion DOFs.

6. Conclusions

A task-oriented type synthesis method for the lower-

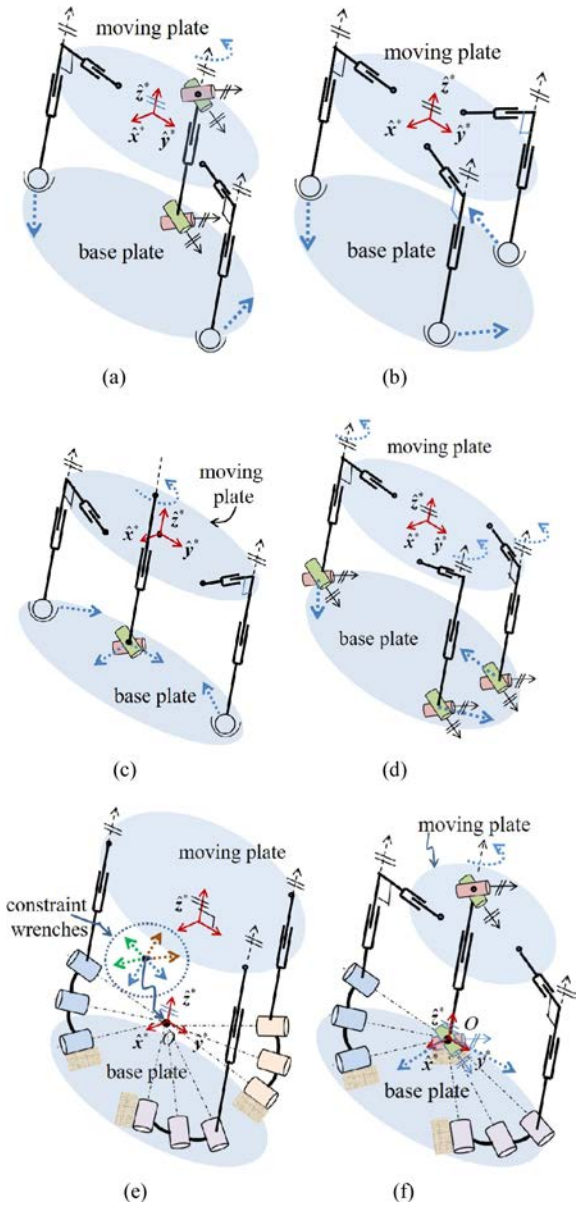

Fig. 14. The $1T_{z^*}2R_{x^*y^*}$ type spatial 3-DOF PMs with three limbs: (a) With two F_{x^*}- limbs and one C_{z^*}- limb; (b) with three two F_{x^*}- limbs; (c) with two F_{x^*}- limbs and one $F_{x^*y^*}C_{z^*}$- limb; (d) with three $F_{x^*}C_{z^*}$- limbs; (e) with three $F_{x^*y^*}$- limb; (f) other version of PM in (a) with the same base point of all three limbs.

mobility PMs with a common platform is suggested, where the task-oriented output motions of the PMs are categorized as $mTnR$ types (m- DOF translational motion and m- DOF rotational motion). In the proposed method, the mechanism constraint set corresponding to the desired output motion of the PM along with its equivalent constraint sets are found and properly distributed to the limbs. Then admissible joint structures of the various types of the constrained limbs required for the task-oriented type synthesis are identified, employing the reciprocal screw conditions. To clearly show the detailed process of the proposed type synthesis method and to verify its effectiveness, type synthesis of three exemplary lower-mobility PM types such as planar $1T_{y^*}$ type, spatial $2T_{x^*y^*}$- type, and spatial $1T_{z^*}2R_{x^*y^*}$ type, are conducted. Not all admissible structures for those three exemplary PMs are enumerated as synthesis results, but several selected and/or new symmetric/asymmetric PM structures are suggested. Based on these results, it can be concluded that the suggested method is not only systematic but also practical to easily conceive the most adequate structures of the PM with the desired output motions.

In this work, the synthesis on the $mTnR$ type PMs are addressed. However, the method could be employed to conduct the synthesis on the PM with any other general form of output motions. Secondly, the PMs employing only revolute joints and/or prismatic joints are considered. However, the method is general such that it can be applied to conducting the synthesis of the lower-mobility PMs consisting of other types of joints such as helical joint, or other generalized kinematic pairs such as planar parallelogram.

Acknowledgments

This work was supported by a Korea University Grant.

Nomenclature

(x^*, y^*, z^*)	: Rotating output reference frame axes
(x, y, z)	: Non-rotating output reference frame axes
$2T_{xy}1R_z$	: 2-*DOF* translational motion on the *x*–*y* plane and 1-*DOF* rotational motion
$F_{xy}C_{y^*}$	: Force constraints along the x- and y- axes and moment constraint around the y^*- axis
$R_{x^*y^*}$	: Rotational motion around the x^*- and the y^*- axes
R_x	: Rotational motion around the z- axis, or revolute joint whose axis is parallel to the z- axis
R_{L^*}	: Revolute joint, the axis of which intersects the z^*- axis
R_{zIx^*}	: Revolute joint, the axis of which is parallel to the z- axis and intersects the y^*- axis
$(R_{u^*}R_{v^*})_{Nz^*}$	: Two revolute joints whose axes intersect at point N on the z^*- axis
$\$_{M0i}$	: Mechanism twist with zero pitch
$\$_{L\infty i}$	: Limb twist with infinite pitch
$\hat{\$}^r_{L0i}$	: Unit mechanism wrench with zero pitch
$\hat{\$}^r_{M\infty i}$	: Unit mechanism wrench with infinite pitch
$\hat{z}^*$	: Screw axis of a unit limb screw, $\hat{\$}_{L0i} = \left(\hat{z}^* \quad \boldsymbol{r} \times \hat{z}^*\right)$

References

[1] Z. Huang and Q. C. Li, General methodology for type synthesis of symmetrical lower-mobility parallel manipulators and several novel manipulators, *The International Journal of Robotics Research*, 21 (2) (2002) 131-145.

[2] Z. Huang and Q. C. Li, Type synthesis of symmetrical lower-mobility parallel mechanisms using the constraint synthesis methods, *The International Journal of Robotics Research*, 22 (1) (2003) 59-79.

[3] F. Gao, W. Li, X. Zhao, Z. Jin and H. Zhao, New kinematic structures for 2-, 3-, 4- and 5-DOF parallel manipulator designs, *Mechanism and Machine Theory*, 37 (2002) 1395-1411.

[4] Y. Fang and L. W. Tsai, Structure synthesis of a class of 4-DOF and 5-Dof parallel manipulators with identical limb structures, *International Journal of Robotics Research*, 21 (9) (2002) 799-810.

[5] X. W. Kong and C. M. Gosselin, *Type synthesis of parallel mechanisms,* Springer-Verlag, Berlin, Germany, 33 (2007).

[6] Q. Li, Z. Huang and J. M. Herve, Type synthesis of 3R2T 5-DOF parallel mechanisms using the Lie group of displacements, *IEEE Trans. on Robotics and Automation*, 20 (2) (2004) 173-180.

[7] M. Karouia and J. M. Hervé, Asymmetrical 3-dof spherical parallel mechanisms, *European Journal of Mechanics A/Solids*, 24 (2005) 47–57.

[8] S. Refaat, J. M. Hervé, S. Nahavandic and H. Trinhc, Asymmetrical three-DOFs rotational-translational parallel-kinematics mechanisms based on Lie group theory, *European Journal of Mechanics-A/Solids*, 25 (3) (2006) 550-558.

[9] O. Salgado, O. Altuzarra, V. Petuya and A. Hernandez, Synthesis and design of a novel 3T1R fully-parallel manipulator, *ASME Journal of Mechanical Design*, 130 (4) (2008) 042305 (1-8).

[10] C. C. Lee and J. M. Herve, Type synthesis of primitive Schoenflies-motion generators, *Mechanism and Machine Theory*, 44 (2009) 1980-1997.

[11] B.-J. Yi, S. M. Kim, H. K. Kwak and W. K. Kim, Multi-task oriented design of an asymmetric 3T1R type 4-DOF parallel mechanism, *Proc. of Mechanical Engineering, Part C: J. of Mechanical Engineering Science*, 227 (10) 2236-2255.

[12] G. Gogu, Structural synthesis of fully-isotropic parallel robots with Schönflies motions via theory of linear transformations and evolutionary morphology, *European Journal of Mechanics A/Solid*, 26 (2007) 242-269.

[13] S. R. Babu, V. R. Raju and K. Ramji, Design optimization of 3PRS parallel manipulator using global performance indices, *Journal of Mechanical Science and Technology*, 30 (9) (2016) 4325-4335.

[14] J. H. Chung, B.-J. Yi and S. Oh, A foldable 3-DOF parallel mechanism with application to a flat-panel TV mounting device, *IEEE Transactions on Robotics*, 25 (5) (2009) 1214-1221.

[15] J. H. Chung, B.-J. Yi, S. H. Lee and W. K. Kim, Implementation of a foldable 3-DOF master device to a glass window panel fitting task, *Automation in Construction*, 19 (7) (2010) 855-866.

[16] S. M. Kim, B.-J. Yi, J. Cheong, M. G. Kim and W. K. Kim, Implementation of a revolute-joint-based asymmetric Schönflies motion haptic device with redundant actuation, *Mechatronics*, 50 (2018) 87-103.

Byung-Ju Yi received the B.S. degree from Hanyang University, Seoul, Korea, in 1984, and the M.S. and Ph.D. degrees from The University of Texas at Austin (UT), TX, USA, in 1986 and 1991, respectively, in mechanical engineering. He served as a Postdoctoral Fellow in the Robotics Group at UT and worked for the Department of Mechanical and Control Engineering, Korea Institute of Technology and Education, Chungnam, Korea. Since 1995, He has been a Professor at the Department of Electronic Systems Engineering, Hanyang University, Ansan, Korea. His research interests include robot mechanics with application to surgical robotic systems and ubiquitous sensor network-based robotics.

Wheekuk Kim received the B.S. degree in mechanical engineering from Korea University, Korea, in 1980, and the M.S. and Ph.D. degrees in mechanical engineering from the University of Texas at Austin, Austin, TX, USA, in 1985 and 1990, respectively. Since 1991, he has been working as a Professor at the Department of Control and Instrumentation Engineering, Korea University, Sejong, Korea. His research interests are in the area of design of parallel robots, synthesis on both the parallel mechanisms and cable-driven parallel mechanisms, and kinematic/dynamic modeling and analysis of parallel robots.